PROPOSAL AND ANALYSIS OF A POPULATION DYNAMICS MODEL OF THE PUBLIC GOODS DILEMMA IN AN ANT COLONY

Santiago Vladimir Gómez Rosero

Dissertação de Mestrado apresentada ao Programa de Pós-graduação em Engenharia Elétrica, COPPE, da Universidade Federal do Rio de Janeiro, como parte dos requisitos necessários à obtenção do título de Mestre em Engenharia Elétrica.

Orientadores: Amit Bhaya
Frederico Caetano Jandre de Assis Tavares

Rio de Janeiro
Abril de 2015

PROPOSAL AND ANALYSIS OF A POPULATION DYNAMICS MODEL OF THE PUBLIC GOODS DILEMMA IN AN ANT COLONY

Santiago Vladimir Gómez Rosero

DISSERTAÇÃO SUBMETIDA AO CORPO DOCENTE DO INSTITUTO ALBERTO LUIZ COIMBRA DE PÓS-GRADUAÇÃO E PESQUISA DE ENGENHARIA (COPPE) DA UNIVERSIDADE FEDERAL DO RIO DE JANEIRO COMO PARTE DOS REQUISITOS NECESSÁRIOS PARA A OBTENÇÃO DO GRAU DE MESTRE EM CIÊNCIAS EM ENGENHARIA ELÉTRICA.

Examinada por:

Prof. Amit Bhaya, Ph.D.

Prof. Eugenius Kaszkurewicz, D.Sc.

Prof. Helio Schechtman, Ph.D.

RIO DE JANEIRO, RJ – BRASIL
ABRIL DE 2015

Gómez Rosero, Santiago Vladimir

Proposal and Analysis of a population dynamics model of the Public Goods Dilemma in an Ant Colony/Santiago Vladimir Gómez Rosero. – Rio de Janeiro: UFRJ/COPPE, 2015.

XI, 80 p.: il.; 29, 7cm.

Orientadores: Amit Bhaya
Frederico Caetano Jandre de Assis Tavares

Dissertação (mestrado) – UFRJ/COPPE/Programa de Engenharia Elétrica, 2015.

Bibliography: p. 56 – 58.

1. Biological Modelling. 2. Public Goods Dilemma. 3. Populations Modelling. 4. *Pristomyrmex punctatus* Ants. I. Bhaya, Amit *et al.* II. Universidade Federal do Rio de Janeiro, COPPE, Programa de Engenharia Elétrica. III. Título.

Acknowledgement

I take the freedom of expressing my sincere gratitude and appreciation in my native language . . .

Agradezco a la vida, por los chaquiñanes que me ha permitido caminar y el aprendizaje obtenido al transitarlos.

Agradezco a mi “Camilita con cariño”, compañera en esta aventura y que sin su apoyo no hubiese sido posible recorrer este chaquiñan.

Agradezco a mis padres y familia, por todo su apoyo y empuje para continuar el camino.

A los amigos. Donde el corazón siente una falta, una mano amiga aparece.

A los profesores Amit y Frederico, por su paciencia y enseñanzas.

Resumo da Dissertação apresentada à COPPE/UFRJ como parte dos requisitos necessários para a obtenção do grau de Mestre em Ciências (M.Sc.)

UM MODELO DA DINÂMICA DE POPULAÇÕES DO DILEMA DOS BENS PÚBLICOS EM UMA ESPÉCIE DE FORMIGAS

Santiago Vladimir Gómez Rosero

Abril/2015

Orientadores: Amit Bhaya
Frederico Caetano Jandre de Assis Tavares

Programa: Engenharia Elétrica

Neste trabalho, propõe-se o modelo da dinâmica do dilema dos bens públicos numa colônia de formigas da espécie *Pristomyrmex punctatus*, baseado nos resultados dos experimentos de Dobata e Tsuji. A colônia de formigas é constituída por formigas operárias e trapaceiras, além o modelo proposto, baseado em equações diferenciais ordinárias no estilo predador-presa, representa as interações de três variáveis: a população das formigas operárias, a população das formigas trapaceiras e os bens públicos no ninho. O modelo foi programado no iThink modeling & simulation software e simulado para analisar o comportamento do modelo. Os resultados das simulações são similares aos resultados apresentados por Dobata e Tsuji. Também o modelo proposto permite as análises do sistema em longo tempo com variações nas proporções de populações iniciais das trapaceiras e das operárias. Além disso é possível determinar a coexistência no ponto de estabilização das populações permitindo a sobrevivência da colônia no tempo sob certas condições.

Abstract of Dissertation presented to COPPE/UFRJ as a partial fulfillment of the requirements for the degree of Master of Science (M.Sc.)

PROPOSAL AND ANALYSIS OF A POPULATION DYNAMICS MODEL OF THE PUBLIC GOODS DILEMMA IN AN ANT COLONY

Santiago Vladimir Gómez Rosero

April/2015

Advisors: Amit Bhaya
Frederico Caetano Jandre de Assis Tavares

Department: Electrical Engineering

This disertation proposes a model of the dynamics of the public goods dilemma in an ant colony of the species *Pristomyrmex punctatus*, based on recent experimental results of Dobata and Tsuji. The ant colony is made up of workers and cheaters, and the proposed model, based on predator-prey style ordinary differential equations, represents the interactions between three variables: the worker ant population, the cheater ant population and the public good in the nest. The model ODEs were coded in the iThink modeling & simulation software and simulated to analyse the behavior of the system. The simulation results are qualitatively very similar to the experimental results obtained by Dobata and Tsuji. The proposed model also allows the investigation of the long term behavior of the five short term case studies proposed by Dobata and Tsuji. In addition, it is possible to vary the quantity and proportion of the population of both cheaters and worker ants and observe the results in the simulation, with respect to the coexistence of the two populations and the long term survival of the ant colony.

Contents

List of Figures **ix**

List of Tables **xi**

1 Introduction **1**

2 The Prystomyrmex Punctatus Public Goods Dilemma (P^3G) Model **5**
2.1 Conceptualization of the proposed model 5
2.2 Model construction 7
2.2.1 Brief description of the Dobata-Tsuji experiments 7
2.2.2 Modelling the experimental characteristics reported by Dobata-Tsuji 9
2.2.3 Using Holling type II functions to define the P^3G model 12
2.3 Model with a saturation in the worker population 15
2.4 The *Prystomyrmex Punctatus* Public Goods Dilemma model (P^3G model) 16
2.4.1 Normalizing the public goods 16
2.4.2 Normalization of the worker and cheater populations 18
2.4.3 P^3G model with brood population 19

3 Fitting the P^3G model to experimental data **21**
3.1 Fitting the extended P^3G model to experimental data 21
3.2 Model results vs experimental data 24
3.3 Model with long term restocking 28

4 Algebraic Conditions for Positivity and Stability of the P^3G Model Equilibria **32**
4.1 Formulas for the equilibrium points of the P^3G model 32
4.2 Algebraic conditions for the positivity of the equilibrium points 34
4.2.1 Positivity condition for the equilibrium in the Public Goods . . . 34
4.2.2 Positivity condition for the equilibrium in cheater ant population 35
4.2.3 Positivity conditions for the equilibrium in worker ant population 35

4.3 Local stability conditions for the P^3G model 36
4.3.1 Stability analysis for the origin 37
4.4 Local stability analysis for the P^3G model in absence of cheaters 38
4.4.1 Equilibrium for public goods in the absence of cheaters 39
4.4.2 Equilibrium for the workers in the absence of cheaters 39
4.4.3 Stability analysis in the absence of cheaters 40
4.5 Application of the conditions to the fitted P^3G model 42
4.5.1 Stability Results in Absence of Cheater Ants 43

5 Seeking Coexistence in the P^3G Model 45
5.1 Local stability in the vicinity of the equilibrium points 45
5.2 Achieving coexistence by modifying two parameters at a time 51
5.3 Achieving coexistence by reducing the influence of the cheaters on the workers' reproduction rate 52

6 Conclusions 54

Bibliography 56

A Development of the smooth switching functions used in the proposed model 59

B Materials 61

C Procedure to Estimate and Optimize the Parameters Values 65

D Jacobian Components 69

E Equilibrium points for model without the reproduction inhibition function 70

F Equations in Ithink 72

G Equations and sweep for stability in Berkeley Madonna 76

List of Figures

2.1 Reproduction of figures 1A and 1B from Dobata and Tsuji 8
2.2 Reproduction of figure 2B from Dobata and Tsuji 8
2.3 Behaviors for the reproduction inhibition function $f(\bar{y})$ and the expected behavior of $b_1(\bar{y})$ 10
2.4 Expected behaviors for the starvation function $g(\bar{z})$ and the working force function $\varphi(\bar{z})$ 11
2.5 Behavior of the smooth switching function $h(R)$. 13
2.6 Behaviors for the density dependence $D_{x3}(\bar{x})$ and the worker population with density dependence 15

3.1 Sketch of the behavior for the populations. 23
3.2 Comparison between the simulation results and the experimental data for both workers and cheaters species. 25
3.3 Simulation results for the extended model. 25
3.4 Envolope of the experimental data from Dobata and Tsuji and simulation results. 26
3.5 Sensitivity of the model to parameter variations. 27
3.6 Comparason between the simulation results of reduced P^3G model and the experimental data for both species. 28
3.7 Simulation for the worker population, cheater population and Public Goods in five cases format. 29
3.8 P^3G model with limiter in absence of cheaters, variation of the term d_{14}. 31
3.9 P^3G model simulations for $d_{14} = 0,001$. 31

5.1 Stability conditions variation for P_1 with sweep of one parameter. 47
5.2 Stability conditions variation for P_2 with sweep of one parameter. 47
5.3 Stability conditions for P_1 setting $d_{21} = 0,026$ and sweeping the parameter b_{11}. 48
5.4 Evolution of the P^3G model with $d_{21} = 0,026$. 49

5.5 Dynamics of the fitted P^3G model with new parameters, $d_{21} = 0,026$ and $b_{11} = 0.01875$ in the vicinity of P_1. 49
5.6 Dynamics of the fitted P^3G model with new parameter values $d_{21} = 0,026$ and $b_{11} = 0,01875$ in five cases format. 50
5.7 Dynamics of the fitted P^3G model with new parameters values $d_{21} = 0,026$ and $b_{11} = 0,03$ in five cases format. 51
5.8 Dynamics of the model with workers uninfluenced by the cheaters with parameters $d_{21} = 0,026$ and $b_{11} = 0,01875$ in five cases format. 53

A.1 Behavior of the switching functions. 59
A.2 Behavior of the smooth switching function $h(R)$. 60

B.1 Implementation of the P^3G model (2.31) in Ithink main and functions. . 62
B.2 Implementation of the P^3G model (2.31) in Ithink population modules. . 62
B.3 Simulation interface to estimate the parameters of the P^3G model in Ithink. 63
B.4 Genetic algorithms tool interface to optimize the estimation of the parameters. 63
B.5 Berkeley Madonna interface to sweep one parameter seeking coexistence. 64

C.1 Comparison between the simulation results and the experimental data first estimation of parameters for both species. 67

List of Tables

3.1 Initial parameters estimated for the P^3G model. 22
3.2 Estimated values for the parameters in the P^3G model and the value of the objective function $E(p)$ calculated. 24
3.3 Allowed variation of the parameters values in the P^3G model fitted with respect to the dynamics of Dobata and Tsuji 26
3.4 Estimated values for the reduced set of parameters in the P^3G model, and the objective function $E(p)$ calculated. 28

4.1 Summary of the equilibrium points for the P^3G model. 43

C.1 Workers population values for the experiments of Dobata and Tsuji . . . 65
C.2 Offspring of the workers values for the experiments of Dobata and Tsuji . 65
C.3 Cheater population values for the experiments of Dobata and Tsuji . . . 66
C.4 Offspring of the workers values for the experiments of Dobata and Tsuj . 66
C.5 Offspring for the workers values for the experiments of Dobata and Tsuji 67
C.6 Offspring for the workers values for the experiments of Dobata and Tsuji 67

Chapter 1

Introduction

There has been long-standing interest in the widespread situation in which costs, from an action by a member of a group, are private, but the benefits are borne by all members of the group. In a biological context, this situation is described by saying that public goods are created by group members at some individual cost, in the expectation that cooperation will develop around them. Indeed, biologists have noticed that cooperation is frequently present in nature (see [1] and refs. therein).

However, the biologist Hardin, in a much cited paper [2], predicted that cheaters, who benefit from public goods without paying for them, will lead to the collapse of cooperation, and this is now referred to in game theory as "the tragedy of the commons" or "the public goods dilemma". There is also experimental evidence, for interactions between viruses and cells, showing that the public goods dilemma can occur and be linked to genetic background. At the level of higher and more complex organisms, there has been little reported work. Dobata and Tsuji [3] provided experimental evidence for the existence of the public goods dilemma in the asexual ant species *Pristomyrmex punctatus* (henceforth *P. punctatus*), occurring between workers (cooperators) and cheaters (free riders). In this species, all workers carry out cooperative as well as asexual reproduction tasks, whereas cheaters (genetically different) reproduce themselves at a rate higher than the workers, without involving themselves in any cooperative tasks. In laboratory experiments, Dobata and Tsuji [3] showed that cheaters were more successful in surviving and reproducing, causing the collapse of cooperation, thus demonstrating the emergence of the public goods dilemma in a non-microbial society. Elucidation of conditions under which cooperation flourishes or collapses is an important and current topic in evolutionary biology.

Prior to the Dobata-Tsuji experiments, the public goods dilemma has been tested experimentally at human level [4], for vertebrate animals [5], and for many microorganisms [6], [7]. It should also be pointed out that Hardin's dire predictions, have been contested by game theorists studying outcomes of noncooperative games in situations where a good

is shared by all players (see Diekert's review [8]), although there is a consensus that all the controversy and discussion centred around the tragedy of the commons has clarified the mechanisms of collective action problems and even suggested ways to overcome them. In this work, we limit ourselves to modeling and studying aspects of the phenomenon that has been shown to exist in the *P. punctatus* species.

Dynamics of the Public Goods Dilemma

The public goods dilemma game can be described in more detail as follows. Assume that the population of an environment can be subdivided into cooperators and cheaters, sometimes also called defectors. The public goods are produced at some cost to each individual cooperator, but once they are produced are available for the whole population in the game, i.e., for the cooperators and the cheaters. The cheater population consumes the public goods without paying its cost or participating in its production. Given this advantage, in time the cheater population attains higher average fitness than the cooperators [9]. Eventually this advantage becomes tragedy, since the cheaters with better fitness begin to overrun the cooperator population and finally, without a sufficient quantity of public goods for the support of the society, both populations become extinct.

Quoting Nowak [1]: " Evolution is based on a fierce competition between individuals and should therefore reward only selfish behavior. Yet we observe cooperation on many levels of biological organization. Genes cooperate in genomes. Cells cooperate in multicellular organisms. There are many examples of cooperation among animals." In short, while competition is the base for evolution of a species, cooperation could be the key for the evolution of societies. Remarkably, when the whole population is composed only of cooperators, the fitness is even higher than when the cheaters are mixed with the cooperators and, in the case that the whole population is made up of cooperators, it is able to persists in time. For populations composed only of cheaters, fitness diminishes greatly and they become extinct more quickly[1].

In order to model the dynamics of the interaction between the worker and cheater ants that are involved in the public goods game, ordinary differential or difference equations are the tool of choice. In this work, the Lotka-Volterra predator-prey equations, as modified by [10], are used as the starting point to develop the proposed model. The actual development of the model also used the systems dynamics approach, pioneered in [11], as well as associated software tools.

Brief description of a Pristomyrmex punctatus ant species

Ants are still objects of much contemporary research since they are one of the social insects more successful in nature, given their adaptation to different environments and their societal structure [12]. One characteristic of great research in this kind of insect is the high level of altruism, where only one caste (queen) engages in reproductive tasks, while the other castes (normally the rest of the colony) engages in the hard work of maintaining the colony and supporting the reproductive caste and their brood (see Gordon [13]). One species of ant that does not require a caste of queens for reproduction, is *P. punctatus*, for which the workers reproduce through the younger intranidal workers and later become extranidal workers, (see Nishide [14]).

Dobata and Tsuji [3] provide experimental evidence for the public goods dilemma in *P. punctatus*. In this species, all workers cooperate on tasks that benefit the whole colony and are also capable of asexual reproduction. However, the colony can be invaded by mutant genetic cheaters that can subvert the division of labor by reproducing themselves, without cooperating on tasks that benefit all. Dobata and Tsuji mention that there are temporal castes among workers and that cheaters engage in "few tasks except for reproduction". For simplicity in this work, we will assume that cheaters do not engage in any tasks other than reproduction and that the temporal caste structure can be represented by a constant proportion of workers (the younger ones) assigned to inside-nest tasks (reproduction and brood care), and the remainder (older workers) assigned to outside-nest tasks (foraging).

Objectives of this dissertation

- Development of a mathematical model of the dynamics of *P. punctatus* ants.
- Verification that the proposed model is capable of emulating the public goods dilemma.
- Fitting of the proposed model to the experimental data of Dobata and Tsuji.
- Examination of conditions and model parameter values that permit coexistence of cheaters and cooperators.

Structure of this dissertation

Chapter 2 describes the development of a model, which is closely based on a two-predator, one-prey model proposed by Elhanati et al. earlier, in a different context. The reported behavior of *P. punctatus* ants is used to propose the modification of the Elhanati model.

Chapter 3 deals with simulation as well as fitting the proposed model to Dobata's real experimental data. Chapter 4 studies stability aspects of the proposed model both in presence and absence of cheaters ants. Finally, Chapter 5 seeks which parameters could be modified in order to gain coexistence between the populations. Chapter 6 is reserved for the conclusions of the dissertation.

Chapter 2

The Prystomyrmex Punctatus Public Goods Dilemma (P^3G) Model

The model of an asexual ant society proposed in this dissertation is a modification of the model proposed in [10, 15] for two populations and one common resource or public good. One of the species called worker ants is the producer of the resource and the other called cheater ants an opportunist. The proposed modifications have the objective of reproducing the characteristics reported in the experiments performed by Dobata and Tsuji [3]. It is also known from the studies of Gordon [16] and Greene [17] that worker ants provide a recruitment force to produce public goods whenever they are scare, and this fundamental characteristic of ants is also a feature of the proposed model. We will standardize our terminology, referring to cooperators and free-riders in a general discussion and respectively to workers and cheaters, when referring to ants.

2.1 Conceptualization of the proposed model

In general terms, the proposed model is composed of three variables, and is based on Lotka-Volterra models for competition of two predators consuming one prey so that, the general model consists of three coupled-nonlinear differential equations.

$$\begin{aligned} \dot{\bar{x}}(t) &= F\left(\bar{z}(t)\right)\bar{x}(t) \\ \dot{\bar{y}}(t) &= G\left(\bar{z}(t)\right)\bar{y}(t) \\ \dot{\bar{z}}(t) &= H\left(\bar{x}(t), \bar{y}(t), \bar{z}(t)\right) \end{aligned} \tag{2.1}$$

where $\bar{x}(t)$, $\bar{y}(t)$ and $\bar{z}(t)$ are respectively, the worker ant population, the cheater ant

population and the public goods, at time t. From now on we will suppose that $t \geq 0$, and t will be suppressed for brevity. Observe that, in this document the terms workers and cheaters are used to denote, respectively, the producer and non-producer populations in accordance with the cited literature. However other terms such as producers and consumers are also used in other contexts.

The functions $F(\bar{z})$ and $G(\bar{z})$ represent the growth rates for each population, influenced, amongst other factors by production and consumption of public goods in the environment. The function $H(\bar{x}, \bar{y}, \bar{z})$ represents the growth rate of the public goods, also affected by the production and consumption of the public goods, as well as population densities.

The Public Goods, abbreviated to PGs from now on, represent all the goods necessary for maintenance and growth of the ant population, aggregating three main activities: nest maintenance, brood care and the search for food. It is important to remark that the experimental nests constructed in the laboratory by Dobata and Tsuji, were provided with a constant supply of food each day, so that, in the specific case of their experiments, the food gathering activity is not part of the public goods.

Elhanati and Schuster [10] propose a model for two micro-organisms, called phenotypes: one produces the resources or public goods and the other does not, just as observed by Dobata and Tsuji. The simplified model equations for resource extraction by two phenotypes proposed in [10] is shown below,

$$\begin{aligned} \dot{\tilde{u}} &= \left(\tilde{\mu}_u(\tilde{s}) - \tilde{D}_u\right)\tilde{u} - \tilde{b}_1\tilde{u} + \tilde{b}_2\tilde{v} \\ \dot{\tilde{v}} &= \left(\tilde{\mu}_v(\tilde{s}) - \tilde{D}_v\right)\tilde{v} + \tilde{b}_1\tilde{u} - \tilde{b}_2\tilde{v} \\ \dot{\tilde{s}} &= \tilde{c}\frac{\tilde{u}}{\tilde{u}+\tilde{z}} - \frac{1}{\tilde{Y}_u}\tilde{\mu}_u(\tilde{s})\tilde{u} - \frac{1}{\tilde{Y}_v}\tilde{\mu}_v(\tilde{s})\tilde{v} \end{aligned} \tag{2.2}$$

where $\tilde{u}$, $\tilde{v}$ are the concentrations of the producer and non-producer phenotype populations respectively, $\tilde{s}$ is the limiting resource concentration, $\tilde{\mu}_i(\tilde{s})$ are the specific growth rates, $\tilde{D}_i$ the death rates, $\tilde{b}_i$ the transition rates between the phenotypes, $\tilde{c}$ and $\tilde{z}$ constants of the reproduction function and $\tilde{Y}_i$ the yield for each phenotype (see [10] for further details).

In the model studied in this dissertation, since worker ants cannot change their species from worker to cheater and vice versa, the terms $\tilde{b}_1$ and $\tilde{b}_2$ are suppressed. In addition, the saturation function in the PGs production, the term $\dfrac{1}{\tilde{u}+\tilde{z}}$, is replaced by a term representing the working force function $\varphi(\cdot)$, which takes into account the recruitment of ants, mentioned by Gordon [16], that occurs when PGs fall below a certain level. Thus

rewriting the model (2.2) in new notation after these modifications yields:

$$\begin{aligned}
\dot{\bar{x}} &= (B_x(\bar{z}) - D_x)\,\bar{x} \\
\dot{\bar{y}} &= (B_y(\bar{z}) - D_y)\,\bar{y} \\
\dot{\bar{z}} &= C_z(\varphi(\cdot))\bar{x} - \frac{1}{Y_x}B_x(\bar{z})\bar{x} - \frac{1}{Y_y}B_y(\bar{z})\bar{y}
\end{aligned} \tag{2.3}$$

Each term in the above equation will be chosen in order to model the reported behavior of the *P. punctatus* ants and is explained in detail in section 2.2.3.

In order to simplify the model and the notation further, the terms $B_i(\bar{z})$ are defined as:

$$\begin{aligned}
B_x(\bar{z}) &= b_1 c_2 \bar{z} \\
B_y(\bar{z}) &= b_2 c_3 \bar{z}
\end{aligned} \tag{2.4}$$

where the products $c_i\bar{z}$ represent the consumption of the PGs in the equation for $\bar{z}$. The terms b_i are the rates of conversion of the PGs consumed by members of the respective species. The yield terms Y_i, are substituted by the terms b_i of each species, in the terminology of [10].

2.2 Model construction

Some specific phenomena observed in the experiments performed with the *P. punctatus* [3], are essential for the characterization of the proposed model. Three principal phenomena are described: the reproduction rate of the workers ants is strongly reduced in the presence of cheater ants; the working force variation (i.e., the recruitment of the workers) is driven by the level of PGs; and finally the cheaters display a strong dependency on the PGs.

2.2.1 Brief description of the Dobata-Tsuji experiments

Dubata and Tsuji [3] developed their experiments with a initial set up of 25 artificial nests of *P. punctatus* in the laboratory. Each colony was composed initially of 100 individuals, varying the proportion of the cheater ants to be 0%, 25%, 50%, 75% and 100%. They divided the experiment into five main cases, each one made up of five colonies. Case 0: 100 worker ants; Case 1: 75 worker ants, 25 cheater ants and so on until the Case 4 with 100 cheater ants, and zero worker ants.

All the colonies started with zero offspring and the experiments lasted 64 days, after which the colonies were frozen and the species of the broods determined.

During the experiment, the colonies were fed with a daily supply of food and the

quantity of ants in outside-nest activities before the feeding time was registered. Additionally the state of cleanliness of the nests was measured periodically, and all the dead ants found were removed and registered. Following this procedure, the results obtained are presented in figure 2.1 and figure 2.2, reproduced from [3], were obtained.

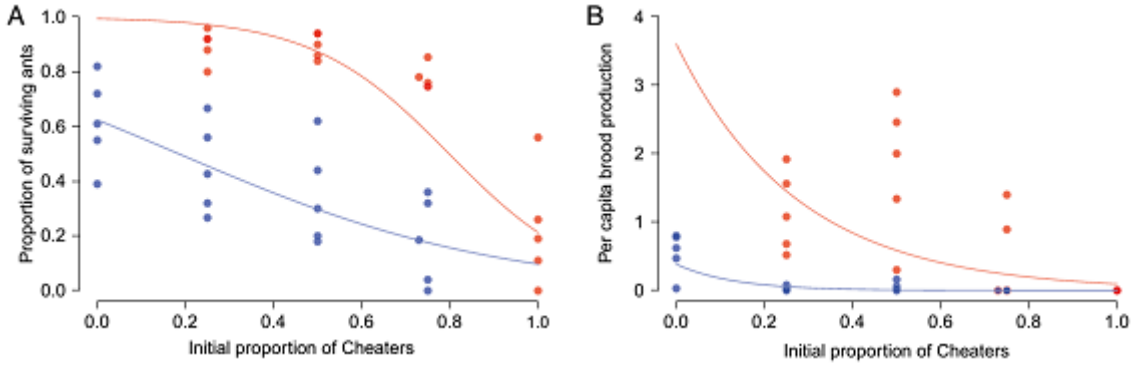

Figure 2.1: Reproduction of figures 1A and 1B from [3]. Showing fitness components of cheaters (red) and workers (blue). (A) survival rate; (B) number of broods per capita

.

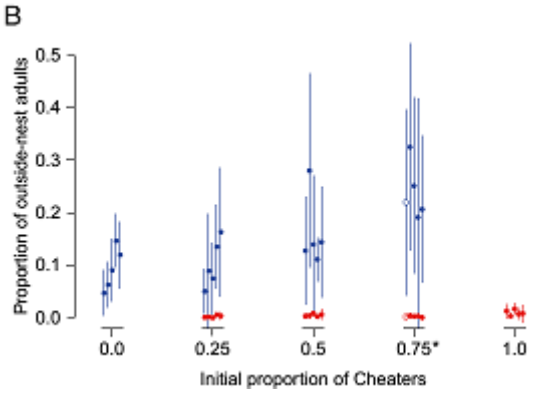

Figure 2.2: Reproduction of figure 2B from [3]: Showing proportional allocation to outside-nest activity. Each dot corresponds to an experimental colony, cheater ants (red) and worker ants (blue).

Graph A in Fig. 2.1, shows the proportion of survivors of both ant species after 64 days, subdivided into the five cases. Graph B in Fig. 2.1 shows the brood production per capita (the reproduction state) for both ant species after 64 days of rearing. Figure 2.2, shows the proportion of outside-nest adults registered in the experiment, each point representing the mean for each experimental colony in each case.

2.2.2 Modelling the experimental characteristics reported by Dobata-Tsuji

Reproduction of workers

Graph B in Fig. 2.1 shows the reproduction rate for both ant species. In the curve corresponding to the worker ant reproduction, it is noticeable that two behaviors occur. In the absence of cheater ants (Case 0), workers exhibit a normal reproduction rate, meaning that the young workers engender their own offspring (lay eggs and breed the larvae), while the older workers take care of the hard work, such as the outside nest tasks and nest maintenance.

In contrast, in the presence of cheater ants in the nest, the workers abandon their reproductive tasks (almost zero eggs laid in Cases 1,2,3), and engage only in brood care activities, nest maintenance and reinforcement of the activities outside the nest.

To model this characteristic, a switching function driven by the presence of cheater ants is proposed. Assume that b_1 is a constant worker growth rate in absence of cheater ants. In the presence of the cheaters in the nest, the workers reduce their reproduction rate, thus the expected behavior is:

$$b_x(\bar{y}) = \begin{cases} b_{11} + b_{12}, & \text{if } \bar{y} = 0 \\ b_{11}, & \text{if } \bar{y} > 0 \end{cases} \tag{2.5}$$

Using the smooth switching function (see section 2.2.3), the required behavior is modeled by the function:

$$b_1(\bar{y}) = b_{11} + \frac{b_{12}}{1 + \bar{\alpha}_2 \bar{y}}$$

The final expression for $b_1(\bar{y})$ is written as:

$$b_1(\bar{y}) = b_{11} + b_{12} f(\bar{y})$$

introducing the notation,

$$f(\bar{y}) = \frac{1}{1 + \bar{\alpha}_2 \bar{y}} \tag{2.6}$$

where $f(\bar{y})$ is called the reproduction inhibition function. It is clear that this choice leads to the behaviour expected for b_1 in (2.5), with a smooth switching function $f(\bar{y})$ shown in figure 2.3.

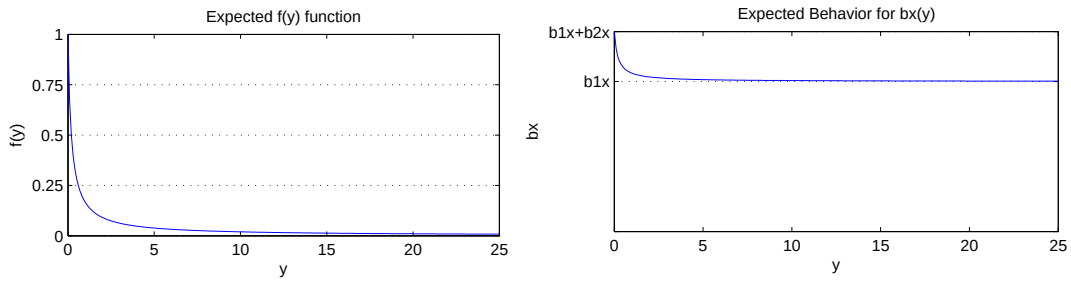

Figure 2.3: Figure A (left), behavior for the reproduction inhibition function $f(\bar{y})$: near $\bar{y} = 0 \ \rightarrow f(\bar{y}) = 1$, for $\bar{y} \gg 0 \ \rightarrow \ f(\bar{y}) \approx 0$. Figure B (right), expected behavior of $b_1(\bar{y})$.

The working force

The behavior of the working force can be seen in figure 2.2. Dobata and Tsuji take the outside activities as a measure of the amount of work required in the nest. As seen in the graph, the largest amount of work is performed by the worker ants, while the cheater ants almost never appear outside the nest.

Taking Case 0 as base (100% worker ants), the flux of the outside-nest activities represents the normal rate of work required to support a colony made up of only worker ants. When the cheater ants increase in proportion (Cases 1, 2 and 3), the flux of workers outside the nest increases its level, eventually doubling its value(see Case 3 in figure 2.2).

The PGs production term which will be denoted $C_z(\varphi(\cdot)) = c_1\varphi(\cdot)$, can be modeled as the product of a production rate c_1 with the working force and recruitment $\varphi(\cdot)$, which increases the quantity of production of PGs when the latter fall below a certain level.

The behavior required for PGs production term C_z is a fixed production rate when there are enough PGs for normal development of the nest, and an increase or higher recruitment in the production when the PGs decreases, as follows:

$$C_z\left(\varphi(\bar{z})\right) = \begin{cases} c_1 + c_{12}, & \text{if } \bar{z} \approx 0 \\ c_1, & \text{if } \bar{z} > 0 \end{cases} \tag{2.7}$$

Then, following the same logic used for b_1, the behavior for C_z can be written as:

$$C_z\left(\varphi(\bar{z})\right) = \left(c_1 + \frac{C}{1 + \bar{\alpha}_3\bar{z}}\right)$$

Choosing $C = 1$, the production term for the PGs, is written as follows

$$C_z\left(\varphi(\bar{z})\right) = c_z\varphi(\bar{z})$$

with the working force function defined as:

$$\varphi(\bar{z}) = \left(1 + \frac{1}{1 + \bar{\alpha}_3 \bar{z}}\right)$$

The working force function $\varphi(\bar{z})$ represents the variation in the recruitment of the worker ants to produce PGs, which is equal to 1 when the PGs are sufficient for the development of the nest activities ($\bar{z} \gg 0$), and increases to 2 in the worst case, when the PGs levels are near zero ($\bar{z} \approx 0$). The behavior of the $\varphi(\bar{z})$ is plotted in figure 2.4.B.

Observe that there is a strong correlation between outside activities and the death rate for the worker ants. As explained by Dobata and Tsuji, with the increase in the hard work(maintenance of the nest and outside-nest activities), the death rate of the workers increases. This phenomena is observed comparing graph A in figure. 2.1, with figure 2.2. It can be observed that in the cases with increased outside-nest activities (Cases 2 and 3), the proportion of survivors of worker ants decreases rapidly, as asserted by the authors. In order to model this behavior, a death rate term dependent on the working force is added to the workers equation, this term is proposed to be:

$$D_{x2}(\bar{x}, \varphi(\bar{z})) = -d_{12}\varphi(\bar{z})\bar{x} \tag{2.8}$$

where, $-d_{12}$ is the fixed death rate for work in the workers equation, and $\varphi(\bar{z})$ the working force.

Strong cheater survival rate

Cheater ants have a very high survival rate as can be seen from figure 2.1.A. In fact, this graph shows that cheater survival is strongly dependent on the existence of public goods: cases 1, 2, 3 show high survival rate or low death rate; however, when public goods become scarce, the cheaters death rate increases dramatically to a mean of 76%

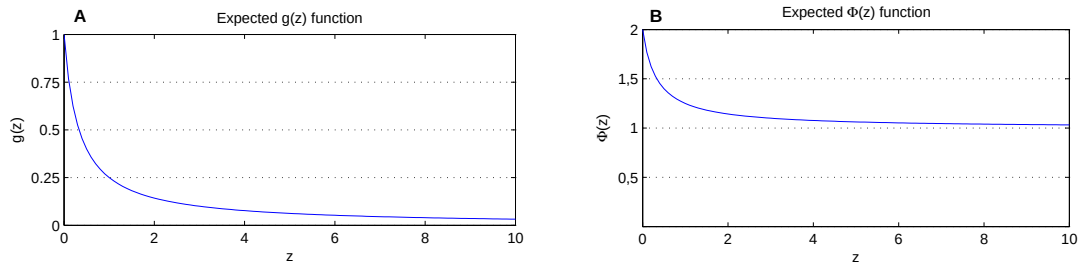

Figure 2.4: Figure A (left), expected behavior for the starvation function $g(\bar{z})$, near to $\bar{z} = 0 \ \rightarrow g(\bar{z}) = 1$ while for $\bar{z} \gg 0 \ \rightarrow \ g(\bar{z}) = 0$. Figure B (right), expected behavior for the working force $\varphi(\bar{z})$ near to $\bar{z} = 0 \ \rightarrow \varphi(\bar{z}) = 2$ while for $\bar{z} \gg 0 \ \rightarrow \ \varphi(\bar{z}) = 1$.

(only 24 cheaters survive after 64 days, from a initial condition of 100). This suggest the use of a switching function which we will call the starvation function:

$$D_{y2}(\bar{z}) = \begin{cases} d_{22}, & \text{if } \bar{z} \approx 0 \\ 0, & \text{if } \bar{z} \gg 0 \end{cases} \tag{2.9}$$

Implementing a smooth function as done for b_1, we propose the term,

$$D_{y2}(\bar{z}) = -\frac{d_{22}}{1 + \bar{\alpha}_3 \bar{z}}.$$

The behavior of the working force function $\varphi(\bar{z})$ and the starvation function $g(\bar{z})$ are shown in figure 2.4. Noticing the $\bar{\alpha}_3$ term existent in $\varphi(\bar{z})$, we unify both smooth switching functions in one for simplicity, as:

$$g(\bar{z}) = \frac{1}{1 + \bar{\alpha}_3 \bar{z}} \tag{2.10}$$

and the starvation function and the working force become respectively,

$$\begin{aligned} D_{y2}(\bar{z}) &= d_{22} g(\bar{z}), \\ \varphi(\bar{z}) &= (1 + g(\bar{z})). \end{aligned}$$

2.2.3 Using Holling type II functions to define the P^3G model

In ecology, smooth switching functions are called Holling type I, II and III functions [18, 19]. In this section we use a modified version of the Holling type II function, which is explained in more detail in the appendix A to represent the smooth switching functions of the previous section. Assume R is the driven variable, then the proposed smooth switching function is defined by:

$$h(R) = \frac{1}{1 + \alpha R} \tag{2.11}$$

α being a parameter of the curve that defines

Figure 2.5 shows the behavior of the smooth switching function, when R is large $h(R)$ tends to zero, while if R tends to zero, then $h(R)$ tends to 1.

The terms $b_1(\bar{y})$ the workers growth rate, D_{y2} as the starvation term and the $\varphi(\bar{z})$ as the working force, all present a switching behavior as explained in section 2.2.2. To meet the required characteristics of (2.5), (2.7) and (2.9) in the model (2.3), it is necessary to introduce some terms in the equations to achieve the expected behavior. Given, the

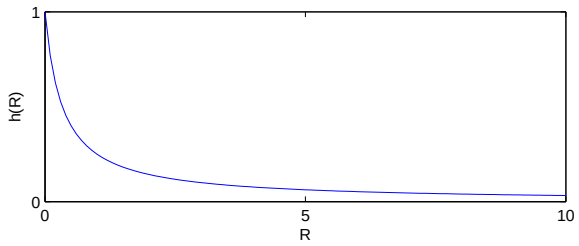

Figure 2.5: Behavior of the smooth switching function $h(R)$.

terms b_1 and D_x are constants and independent of variables $\bar{y}$ and $\bar{z}$ respectively, in the workers equation; the term D_y is constant and independent of the variable $\bar{z}$, in the cheater equation; the PGs production $C_z(\varphi(z))$ requires definition. The terms $B_{x2}(\cdot)$, $D_{x2}(\cdot)$ and $D_{y2}(\cdot)$ were added to (2.3) to proceed with the calculations, as follows:

$$\begin{aligned} \dot{x} &= (b_1 c_2 \bar{z} - D_x)\, x + B_{x2}(\cdot) + D_{x2}(\cdot) \\ \dot{\bar{y}} &= (b_y c_3 \bar{z} - D_y)\, \bar{y} + D_{y2}(\cdot) \\ \dot{\bar{z}} &= C_z(\varphi(\bar{z}))x - c_2 x\bar{z} - c_3 y\bar{z} \end{aligned} \tag{2.12}$$

In order to achieve the behavior for $b_1(\bar{y})$ shown in (2.5),b_1 was renamed as b_{11} and the term $B_{x2}(\cdot)$ defined using a reproduction rate b_{12} accompanied with the smooth switching function in (2.11) dependent on the variable $\bar{y}$, as follows:

$$B_{x2}(x, \bar{y}, \bar{z}) = \frac{b_{12}}{1 + \bar{\alpha}_2 \bar{y}} c_2 \bar{z} x, \tag{2.13}$$

which vanishes when $\bar{y}$ is large enough and is fully operative when $\bar{y}$ is near zero.

The term $D_{x2}(\cdot)$ represents the death rate due to hard work and depends directly on the working force, as explained in subsection 2.2.2, and is modeled by (2.8).

For cheater ants, the term $D_{y2}(\cdot)$ increases the death rate of the cheaters when the PGs are scarce. In order to achieve the behavior in (2.9), this term is constructed similarly to b_1, with a death rate $-d_{22}$ and the function dependent on the variable $\bar{z}$, as follows:

$$D_{y2}(\bar{y}, \bar{z}) = -\frac{d_{22}}{1 + \bar{\alpha}_3 \bar{z}} \bar{y}, \tag{2.14}$$

so that, D_{y2} vanishes when PGs are enough to support the colony, and activates when the PGs are near zero.

To reproduce the switching behavior in (2.7) in the production of the PGs $C_z(\varphi(\bar{z}))$, it was modeled with two production rates, one constant c_1, and the second one called C,

accompanied by the function dependent on the variable $\bar{z}$, as follows:

$$C_z\left(\varphi(\bar{z})\right) = \left(c_1 + \frac{C}{1+\bar{\alpha}_3\bar{z}}\right)$$

choosing $C = c_1$ and simplifying the term, we obtain,

$$C_z\left(\varphi(\bar{z})\right) = c_1\left(1 + \frac{1}{1+\bar{\alpha}_3\bar{z}}\right) \tag{2.15}$$

where, c_1 is the reproduction of PGs rate, and the terms inside the parenthesis represent the working force, i.e., we can also write:

$$C_z\left(\varphi(\bar{z})\right) = c_1\varphi(\bar{z}) \tag{2.16}$$

where,

$$\varphi(\bar{z}) = \left(1 + \frac{1}{1+\bar{\alpha}_3\bar{z}}\right) \tag{2.17}$$

Finally in order to complete the model, with the characteristics mentioned previously, the following terms were substituted into (2.12):

- $B_{x2}(\bar{x},\bar{y},\bar{z}) = \frac{b_{12}}{1+\bar{\alpha}_2\bar{y}}c_2\bar{z}\bar{x}$, defined in (2.13),
- $D_{x2}(\bar{x},\varphi(\bar{z})) = -d_{12}\varphi(\bar{z})\bar{x}$ defined in (2.8),
- $D_{y2}(\bar{y},\bar{z}) = -\frac{d_{22}}{1+\bar{\alpha}_3\bar{z}}\bar{y}$ defined in (2.14),
- $C_z(\varphi(\bar{z})) = c_1\varphi(\bar{z})$ defined in (2.16)
- $D_x = d_{11}$

And after some algebra, we obtain the first attempt at our model proposal:

$$\begin{aligned}
\dot{\bar{x}} &= \left[\left((b_{11} + \frac{b_{12}}{1+\bar{\alpha}_2\bar{y}}\right)c_2\bar{z} - (d_{11} + d_{12}\varphi(\bar{z}))\right]\bar{x} \\
\dot{\bar{y}} &= \left[b_2c_3\bar{z} - \left(d_{21} + \frac{d_{22}}{1+\bar{\alpha}_3\bar{z}}\right)\right]\bar{y} \\
\dot{\bar{z}} &= c_1\varphi(\bar{z})\bar{x} - (c_2\bar{x} + c_3\bar{y})\bar{z}
\end{aligned} \tag{2.18}$$

In the absence of cheater ants, the model (2.18) could have unbounded trajectories, as well as some other undesirable characteristics. This leads to the introduction of a refined version of the model (2.18) in the following section.

2.3 Model with a saturation in the worker population

It is common to encounter growth-limiting factors in real biological systems and these are referred to by names such as overcrowding and carrying capacity (Gurney [20], Edelstein [21] et al), which cause populations to follow a logistic curve which saturates, rather than an exponentially increasing one. Many mathematical models of density dependent growth have been proposed in the literature (see Abrams [22] and Bazykin et al [23]). Several of these were tried, and the choices which resulted in the most reasonable rates are detailed in this section.

An overcrowding term is introduced to the worker equation in order to limit the growth rate. This term reduces the growth rate of the predator $\bar{x}$ and is proportional to its own density, as explained by Abrams [22]. It is defined by:

$$D_{x3}(\bar{x}) = -d_{13}\bar{x}^2 \tag{2.19}$$

where, d_{13} is the additional death rate due to the overcrowding in the nest, and the density dependence is quadratic. The graph and effect of this term on the population dynamics is shown in figure 2.6.

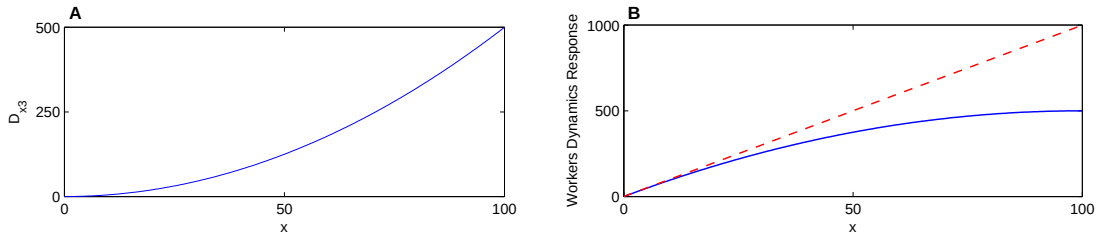

Figure 2.6: Figure A (left), behavior of the worker density dependence $D_{x3}(\bar{x})$ with $d_{13} = 0.05$. Figure B (right), behavior of the worker population: red curve describes growth without the density dependence term (2.19); blue curve shows the effects of introducing the predator density dependence term (2.19) into the predator population growth equation.

The term $D_{x3}(\bar{x})$ is added to the worker equation in the basic model (2.18), in order to obtain the dynamics of the proposal model with an overcrowding limiter, as follows:

$$\begin{aligned}
\dot{\bar{x}} &= \left[\left(b_{11} + b_{12}f(\bar{y})\right)c_2\bar{z} - \left(d_{11} + d_{12}\varphi(\bar{z}) + d_{13}\bar{x}\right)\right]\bar{x} \\
\dot{\bar{y}} &= \left[b_2c_3\bar{z} - \left(d_{21} + d_{22}g(\bar{z})\right)\right]\bar{y} \\
\dot{\bar{z}} &= c_1\varphi(\bar{z})\bar{x} - \left(c_2\bar{x} - c_3\bar{y}\right)\bar{z}
\end{aligned} \tag{2.20}$$

where the functions modelling, respectively are, reproduction inhibition $f(\bar{y})$, starvation $g(\bar{z})$ and working force $\varphi(\bar{z})$, are:

$$f(\bar{y}) = \frac{1}{1 + \bar{\alpha}_2 \bar{y}}; \tag{2.21}$$

$$g(\bar{z}) = \frac{1}{1 + \bar{\alpha}_3 \bar{z}}; \tag{2.22}$$

$$\varphi(\bar{z}) = 1 + g(\bar{z}); \tag{2.23}$$

The interpretations of the 13 parameters in (2.20) are as follows:

- b_{11}: is the conversion rate of PGs into worker growth rate in presence of cheaters,
- b_{12}: is the conversion rate of PGs into an additional worker growth rate given the absence of the cheaters,
- b_2: is the conversion rate of PGs into cheater growth rate,
- d_{11}: is the death rate due to age of the workers,
- d_{12}: is the death rate due to work, of the workers,
- d_{13}: is the death rate due to overcrowding of the workers,
- d_{21}: is the death rate due to age of the cheaters,
- d_{22}: is the cheater death rate due to absence of PGs,
- c_1: is the PGs production rate generated by the workers,
- c_2: is the consumption rate of the PGs by the workers,
- c_3: is the consumption rate of the PGs by the cheaters,
- $\bar{\alpha}_2$: is a factor that define the asymptotic behavior of the function $f(\bar{y})$.
- $\bar{\alpha}_3$: is a factor that define the asymptotic behavior of the function $g(\bar{z})$.

2.4 The *Prystomyrmex Punctatus* Public Goods Dilemma model (P^3G model)

The proposed model was normalized in $\bar{z}$ and scaled in $\bar{x}$ and $\bar{y}$ to facilitate the understanding of its behavior. The ant equations were scaled using the proportion of worker ants or cheaters ants with respect to the total population in the nest. The PGs were normalized to the maximum value that variable can achieve along time, as explained in the next section.

2.4.1 Normalizing the public goods

In order to normalize the PGs, it was necessary to locate the maximum value that can be reached by the variable. Evaluating the five cases using simulations, it was observed

that the PGs reach their steady and maximum value when there are no cheaters in the nest. In this case $\bar{y}(0) \equiv 0$ implying that $\dot{\bar{y}}(0) = 0$ and furthermore that $f(\bar{y}) = 1$ for all $t > 0$. Thus the model reduces to:

$$\dot{\bar{x}}_{nc} = \left[(b_{11} + b_{12})c_2\bar{z}_{nc} - (d_{11} + d_{12}\varphi(\bar{z}_{nc}))\right]\bar{x}_{nc} \tag{2.24}$$

$$\dot{\bar{z}}_{nc} = \left[c_1\varphi(\bar{z}_{nc}) - c_2\bar{z}_{nc}\right]\bar{x}_{nc} \tag{2.25}$$

where, $\bar{x}_{nc}$ and $\bar{z}_{nc}$ are the worker population and PGs respectively, in absence of the cheaters in the nest, (the subscript nc recalls no cheaters).

By setting $\dot{\bar{z}}_{nc} = 0$, the equilibrium points were calculated from the PGs equation in (2.25) as follows:

$$\bar{z}^*_{nc,1,2} = \frac{-(c_2 - \bar{\alpha}_3 c_1) \pm \sqrt{(c_2 - \bar{\alpha}_3 c_1)^2 + 8\bar{\alpha}_3 c_1 c_2}}{2\bar{\alpha}_3 c_2} \tag{2.26}$$

Equation (2.26) shows that there are two possible equilibrium points of which only the positive one is admissible. This positive equilibrium point of the PGs in absence of cheaters, called M, is given by:

$$M = \frac{-(c_2 - \bar{\alpha}_3 c_1) + \sqrt{(c_2 - \bar{\alpha}_3 c_1)^2 + 8\bar{\alpha}_3 c_1 c_2}}{2\bar{\alpha}_3 c_2} \tag{2.27}$$

We claim that M is the maximum value that the PGs can reach.

This is proved as follows. Consider the original model in (2.18) and set $\dot{\bar{z}} = 0$ which leads to:

$$\bar{z}^* = \frac{-\left(c_2 + c_3\frac{\bar{y}}{\bar{x}} - \bar{\alpha}_3 c_1\right) \pm \sqrt{\left(c_2 + c_3\frac{\bar{y}}{\bar{x}} - \bar{\alpha}_3 c_1\right)^2 + 8\bar{\alpha}_3 c_1\left(c_2 + c_3\frac{\bar{y}}{\bar{x}}\right)}}{2\bar{\alpha}_3\left(c_2 + c_3\frac{\bar{y}}{\bar{x}}\right)} \tag{2.28}$$

Taking the positive value of the square root in 2.28 for $\bar{z}$ and denoting this value $M_y(\bar{x}, \bar{y})$, we get:

$$M_y(\bar{x}, \bar{y}) = \frac{-\Delta_y + \sqrt{\Delta_y^2 + 8\bar{\alpha}_3 c_1\left(c_2 + c_3\frac{\bar{y}}{\bar{x}}\right)}}{2\bar{\alpha}_3\left(c_2 + c_3\frac{\bar{y}}{\bar{x}}\right)} \tag{2.29}$$

where

$$\Delta_y = \left(c_2 + c_3\frac{\bar{y}}{\bar{x}} - \bar{\alpha}_3 c_1\right).$$

Clearly, if $\bar{y} = 0$ and $\bar{x} \neq 0$, $M_y(\bar{x}, \bar{y}) = M$. Note that

$$M_y(\bar{x}, \bar{y}) \simeq \frac{m}{\sqrt{\left(c_2 + c_3 \frac{\bar{y}}{\bar{x}}\right)}}$$

where

$$m = \sqrt{\frac{2c_1}{\bar{\alpha}_3}}$$

Thus if $\bar{y} = 0$,

$$M_y(\bar{x}, 0) = M = \frac{m}{\sqrt{c_2}}$$

For positive populations of workers and cheaters, it holds that:

$$\frac{1}{\sqrt{c_2}} > \frac{1}{\sqrt{\left(c_2 + c_3 \frac{\bar{y}}{\bar{x}}\right)}}$$

which means that $M > M_y(\bar{x}, \bar{y})$

Thus for any positive value of $\bar{x}$ or $\bar{y}$ the value of $M_y(\bar{x}, \bar{y})$ is less than M, as claimed.

2.4.2 Normalization of the worker and cheater populations

The idea behind the experimental nests in [3] is to use an initial total number of 100 ants, with different proportions of the two interacting populations. Thus the populations $\bar{x}$ and $\bar{y}$ are scaled with respect to the initial total population in the nest. Denote the total population of the nest as:

$$N(t) = \bar{x}(t) + \bar{y}(t)$$

and the initial setup of the nest as:

$$N_0 = \bar{x}(0) + \bar{y}(0)$$

In order to normalize-scale the model, new variables are defined as:

$$x(t) = \frac{\bar{x}(t)}{N_0}; \quad y(t) = \frac{\bar{y}(t)}{N_0}; \quad z(t) = \frac{\bar{z}(t)}{M}; \tag{2.30}$$

The new model called from now on of *P. punctatus* public goods dilemma model in short P^3G model, is obtained by substituting the new variables defined in (2.30) into

(2.20), obtaining.

$$\begin{aligned}
\dot{x} &= \left[\left(b_{11} + b_{12} f(y)\right) c_4 \rho_M z - \left(d_{11} + d_{12}\varphi(z) + d_{14} x\right)\right] x \\
\dot{y} &= \left[b_2 c_5 \rho_M z - \left(d_{21} + d_{22} g(z)\right)\right] y \\
\dot{z} &= c_1 \varphi(z) \rho_M^{-1} x - \left(c_4 x + c_5 y\right) z
\end{aligned} \tag{2.31}$$

And the new reproduction inhibition function, starvation function and working force function, respectively are:

$$f(y) = \frac{1}{1 + \alpha_2 y}; \tag{2.32}$$

$$g(z) = \frac{1}{1 + \alpha_3 z}; \tag{2.33}$$

$$\varphi(z) = 1 + g(z); \tag{2.34}$$

and the new parameters are defined as:

$$\rho_M = \frac{M}{N_0}; \quad c_4 = c_2 N_0; \quad c_5 = c_3 N_0; \quad d_{14} = d_{13} N_0; \quad \alpha_2 = \bar{\alpha}_2 N_0; \quad \alpha_3 = \bar{\alpha}_3 M; \tag{2.35}$$

2.4.3 P^3G model with brood population

In order to estimate the parameters of the model (2.31), is necessary to fit the simulation results in $t = 64$ of the model to the experimental data presented by Dobata and Tsuji in [3]. To do this first note that the experimental data contains information on the brood populations, as well as the survivors (of both of cheaters and workers) at the end of a sixty-four day time period, while the P^3G model introduced in the previous section only considered the adult populations. To solve this issue is introduced two additional differential equations, which bookkeep the evolution of the two brood populations.

The experimental data reported by Dobata and Tsuji [3] are reported after 64 days of evolution from the initial population, in each of the five cases studies given. As Tsuji [24] point out, this is not long enough to allow an egg to give rise to a productive adult. For this reason, we propose to include two differential equations to the P^3G model that account for the growth of a brood population but are decoupled from the three P^3G equations, since reposition for adults does not occur in the short horizon of 64 days. In accordance with the data in [3], we will lump together, in the offspring population, eggs, pupae and larvae. This leads to the following extended P^3G model which is actually

fitted to the experimental data:

$$\begin{aligned}
\dot{x}_1 &= \left[(b_{11,adult})c_4\rho z - (d_{11} + d_{12}\varphi(z) + d_{14}x_1)\right] x_1 \\
\dot{x}_2 &= \left(b_{11,offs} + b_{12}f(y)\right) c_4\rho z x_1 \\
\dot{y}_1 &= \left[b_{2,adult}c_5\rho z - (d_{21} + d_{22}g(z))\right] y_1 \\
\dot{y}_2 &= b_{2,offs}c_5\rho z y_1 \\
\dot{z} &= c_1\varphi(z)\rho^{-1}x_1 - (c_4x_1 + c_5y_1)z
\end{aligned} \tag{2.36}$$

where x_1, x_2, y_1 and y_2 respectively are, the worker adult population, the offspring of the workers, the cheater adult population and the offspring of the cheaters and z, as usual, denotes PG. The growth rates b_{11} and b_2 are divided into two growth rates, an adult rate $b_{i,adult}$ and the reproduction rate by $b_{i,offs}$. Since Dobata and Tsuji do not give data of dead offspring, the death rate for the offspring equations is suppressed. Recalling, the rate b_{12} is the additional reproduction rate of the workers in absence of the cheaters, then it is included in the offspring equation for the workers.

Chapter 3

Fitting the P^3G model to experimental data

This chapter deals with the problem of fitting the P^3G model, which was inspired by Dobata and Tsuji's description of the behavior of *P. punctatus*, to the actual data provided by them in [3]. There is a problems that arise immediately, is that the experimental data only give the initial and final values of the state variables. In other words, it is necessary to fit the model to a very sparse data set, which contains no intermediate values of the state variables. This problem will be tackled with an optimal control type of approach, which, however, uses a genetic algorithm to find the optimal "control" (i.e., parameters), rather than optimal control theory. In addition, since the number of parameters is quite large, a sensitivity analysis complements the fitting performed by the genetic algorithm, in order to test the model robustness as well as the parsimony of the parametrization.

3.1 Fitting the extended P^3G model to experimental data

When time series data on all the state variables are available, many methods are available, such as one-step-ahead prediction. The difficult problem is to fit mechanistic models when information about state variables is missing.

Model fitting based on one-step-ahead prediction requires time-series measurements for all state variables in the model. This is rare in ecological applications and usually models have to be fitted when dynamics of some important variables are unknown. In this case, one general approach is called trajectory matching and because it is conceptually simple and easily programmable, it is often used in ecological applications (see, for e.g. [25, 26]).

Trajectory matching has simple underlying logic, and can be illustrated by the example of fitting a parasitoid-host model to data. Let us suppose that we have only a set of measurements of host data, $\{N_t\}, t = 1, \ldots, n$. Suppose that the model we wish to fit has a vector of parameters that we are interested in estimating. For any particular choice of parameter values and initial host and parasitoid densities, we can solve the model forward for n steps, and obtain the model-predicted sequence $\{\hat{N}_t^*\}$ (the hat superscript denotes values generated by the model). A sequence of parasitoid densities is also obtained but discarded, since no data against which to compare it is available. To calculate the degree of fit between the model predictions and data, some measure, call it E, of the goodness of fit is employed. This defines a mapping from a set of parameters and initial values to E. The next step is to use some standard software for function minimization, and ask it to find the set of parameters and initial values that will minimize E. Of course, one must be extremely careful about using the trajectory-matching approach. With a dynamical system that retains memory of its initial conditions at least for a time comparable to the length of the data series, this approach can give meaningful results [27].

To estimate the 15 parameters in the extended P^3G model (2.36), it is necessary to first describe the behavior of the curves for $t = 64$ days with the characteristics explained before. Consider the equations for the adults for both species, the dynamic for this kind of population will be modeled through a declining curve given they don't receive reposition from the broods.

With regard to the offspring populations, as was explained by Dobata and Tsuji, in the onset of the experiment all the brood was removed. The initial offspring population for all the cases is zero, and given that there is no death term, the dynamic is represented by a growing curve, except for Case 4 (100% cheaters) where the eggs are neglected and all the broods die. To visualize these dynamics, a sketch of the curves was drawn and is shown in the figure 3.1.

With the sketch as guide, we proceeded to estimate the values for the parameters with help of the Ithink software [28] and the Optimization Toolbox in Matlab [29]. The initial parameters were calculated using Ithink. The P^3G model in (2.31) was simulated in iThink (refer to appendix B). The vector of the initial parameters estimated are presented in the table 3.1

Initial Parameters							
$b_{11\ offs}$	$b_{11\ adult}$	b_{12}	d_{11}	d_{12}	d_{14}	$b_{2\ offs}$	$b_{2\ adult}$
0.0001	0.0015	0.0035	0.003	0.0055	0.001	0.02	0.0015
d_{21}	d_{22}	c_1	c_4	c_5	α_2	α_3	
0.001	0.016	1.5	25	25	500	3	

Table 3.1: Initial parameters estimated for the P^3G model.

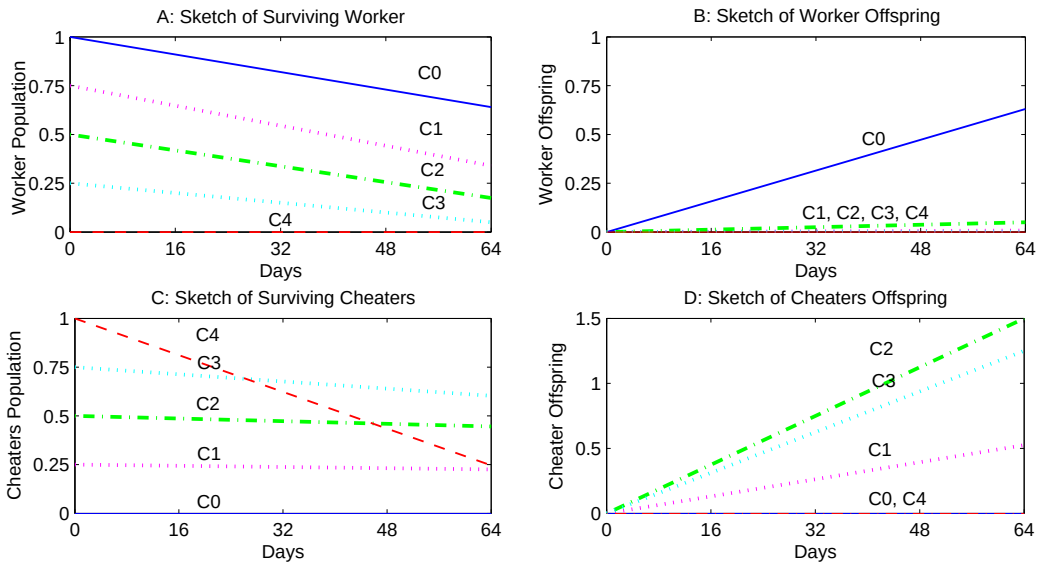

Figure 3.1: Sketch of the behavior for the populations: A: Surviving workers, B: Offspring of the workers, C: Surviving Cheaters and D: Offspring of the Cheaters, over 64 days in five cases arrange. Blue: Case 0, Pink: Case 1, Green: Case 2, Cyan: Case 3 and Red: Case 4.

The simulations of the model with these initial parameters still have deviations with respect to the mean of the experimental results. In order to reduce this error, the Genetic Algorithms optimization tool of Matlab is used, as described below. Consider:

$$\omega(t) = \begin{bmatrix} x_1 \\ x_2 \\ y_1 \\ y_2 \\ z \end{bmatrix} \tag{3.1}$$

In this notation, (2.36) is written as:

$$\dot{\omega}(t) = \psi(\omega, p, t) \tag{3.2}$$

where $\omega \in \mathbb{R}^5$ is the vector of the variables, $p \in \mathbb{R}^{15}$ is the vector of parameters of the P^3G model and $\psi(\omega, p, t)$ the dynamics of the populations in the P^3G model in (2.31). And the solution of 3.2 is written as:

$$\omega(t) = \Psi(t, t_0, \omega, p) \tag{3.3}$$

consider the results of 3.3 evaluated for $t \in [0, 64]$ and defined for each experimental case

by i=0,1,2,3,4, as follows:

$$\omega^i(64) = \Psi(64, 0, \omega_0^i, p) \tag{3.4}$$

where ω_0^i are the initial of conditions of 3.2 in $t = 0$.
Thus the objective function is constructed under the LSE philosophy as follows:

$$E(p) = \sum_{i=0}^{4} \left[\Omega_{DT}^i - \omega^i(64)\right]^2 \tag{3.5}$$

where $E(p)$ represents the objective function dependent to be minimized, Ω_{DT} are the experimental results of Dobata and Tsuji after 64 days. Finally substituting 3.4 into 3.5 we obtain the objective function to be optimized, defined as:

$$E(p) = \sum_{i=0}^{4} \left[\Omega_{DT}^i - \Psi(64, 0, \omega_0^i, p)\right]^2 \tag{3.6}$$

Then this function is minimized with the Genetic Algorithms tool, finding the value of the vector p that minimize the quadratic error, starting from the initial parameters estimated in the table 3.1. With the procedure explained in the appendix C, was obtained the optimized values for the parameters of the P^3G model, shown in the table 3.1.

Parameters	Values	Parameters	Values
b_{11}	0.0147	c_1	1.8
b_{12}	0.0066	c_4	21
d_{11}	0.0119	c_5	10
d_{12}	0.0207		
d_{14}	0.001	α_2	500.01
		α_z	3
b_{21}	0.0442		
d_{21}	0.0009		
d_{22}	0.0242	$E(p)$	0.0977

Table 3.2: Estimated values for the parameters in the P^3G model and the value of the objective function $E(p)$ calculated.

3.2 Model results vs experimental data

Once the parameters have been estimated, we proceed to plot the simulations and the mean of the experimental results to verify the quality of the fit. Allowing to compare the model performance with respect to the experimental data presented by Dobata and Tsuji [3], (see figure 3.2. Additionally figure 3.3 presents the simulations of the evolution of each population and the PGs.

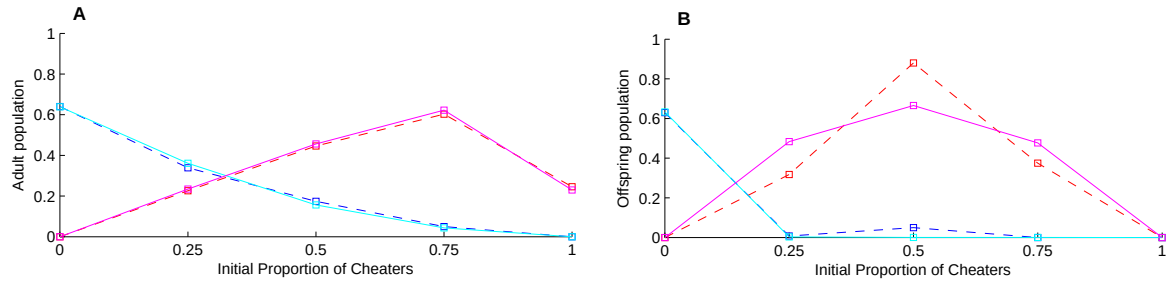

Figure 3.2: Comparision between the simulation results and the experimental data for both the workers and cheaters species. (A):Proportion of surviving adults, (B): Offspring produced. Blue curve workers experimental data, cyan curve workers simulation results, red curve Cheaters experimental data, pink curve Cheaters simulation results.

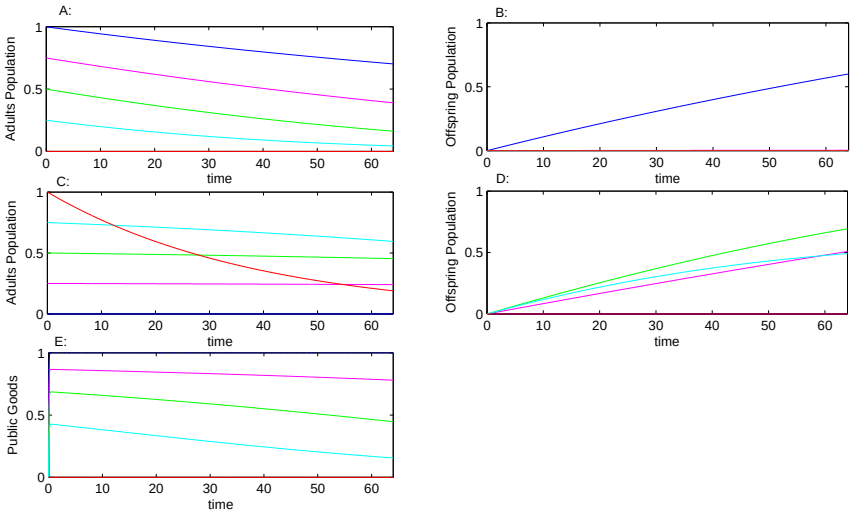

Figure 3.3: Simulation results for the extended model: (A) The adults workers, (B) The offspring of the workers, (C) The adults cheaters, (D) The offspring of the cheaters and (E) The public goods, in five cases format; Blue: Case 0, Pink: Case 1, Green: Case 2, Cyan: Case 3 and Red: Case 4.

Figure 3.2 shows that the results of the simulations for the adult populations fits the experimental data well, with some differences for the cases composed of only one population (case 0 and 4). On the other hand about the worker offspring population closely follows the experimental results, while the simulation for the cheaters shows some difference with the experimental results.

We propose a method to determine the sensibility of the parameters of the fitted model with respect to the parameters. Recall the experimental results are in sets of 25 data points for each population, divided into five cases. In other words, for each case there are 5 experimental results, with a minimum, maximum and a mean value.

Figure 3.4 show plots of the four populations from the experimental results, and the

highlighted region shows the area of the experimental results after 64 days. This region, from now on called the DT envelope for simplicity, is delimited by an upper bound and a lower bound given by the maximum and minimal values of each experimental case.

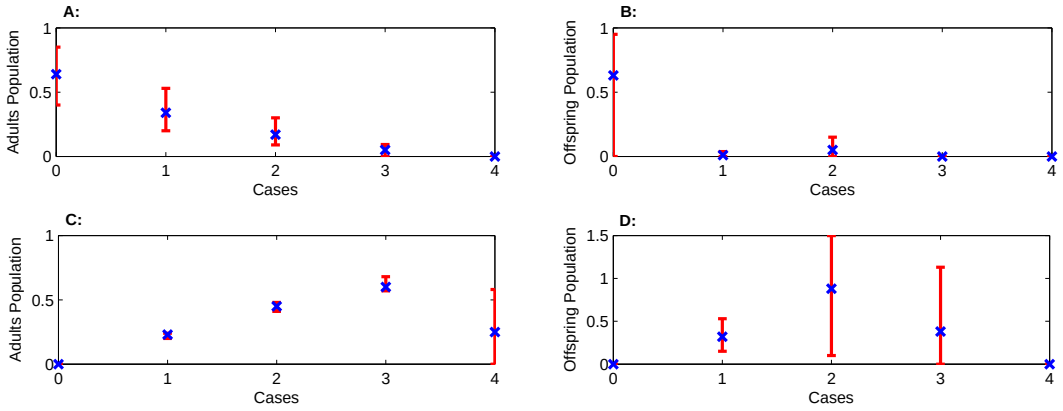

Figure 3.4: Envelope of the experimental data from Dobata and Tsuji and simulation results, (A) The adult workers, (B) The offspring of the workers, (C) The adult cheaters, (D) The offspring of the cheaters. Blue curve: mean of the experimental results, Red curves: maximum and minimal points for each case.

We define the measure of how large the allowed variation of one parameter can be before the simulation result ends up outside the DT envelope, using the initial values of the parameters shown in table 3.1. To achieve this, we use a script in Matlab to sweep one parameter at time in steps of 1% (increasing and decreasing the value), until the simulation result is outside the envelope. The maximum allowed deviations obtained are shown in table 3.3.

Allowed variation of the Parameters					
Responsive		Necessary		Indifferent	
$b_{11\ adult}$	$+19\%$	b_{12}	$+54\%$	$b_{11\ offs}$	$\gg 100\%$
$b_{2\ offs}$	$+11\%$	d_{14}	$\gg 100\%$	d_{11}	-41%
d_{12}	-24%	d_{22}	-69%	$b_{2\ adult}$	$\gg 100\%$
c_1	$+9\%$	α_2	-91%	d_{21}	-38%
c_4	-12%	α_3	-91%		
c_5	$+14\%$				

Table 3.3: Allowed variation of the parameters values in the P^3G model fitted with respect to the dynamics of Dobata and Tsuji

The positive percentages refer to an increase in the original value, while the negative ones refer to a decrease. The parameters with the notation $\gg 100$ are those that can even be doubled in value, but the corresponding simulation remains inside the DT envelope.

Thus large allowed variation in a parameter corresponds to a low sensitivity of the model the parameter.

These sensitivity results show that there exist three sets of parameters whose variation affects, to a greater or lesser extent, the end results of the simulations. The group named as responsive are the more sensitive parameters, meaning, that the range of variation is less than 25%; the groups named necessary and indifferent are the parameters whose allowed variation is greater than 25% before the corresponding simulation fall outside of the DT envelope, "necessary" are the parameters that can not be removed, given that they represent some fundamental characteristics of the model, and, the parameters "indifferent" are possibly dispensable parameters.

As example to visualize the sensitivity of the parameters, figure 3.5 shows the variation of two different parameters and the points where the final result begins to venture outside the DT envelope.

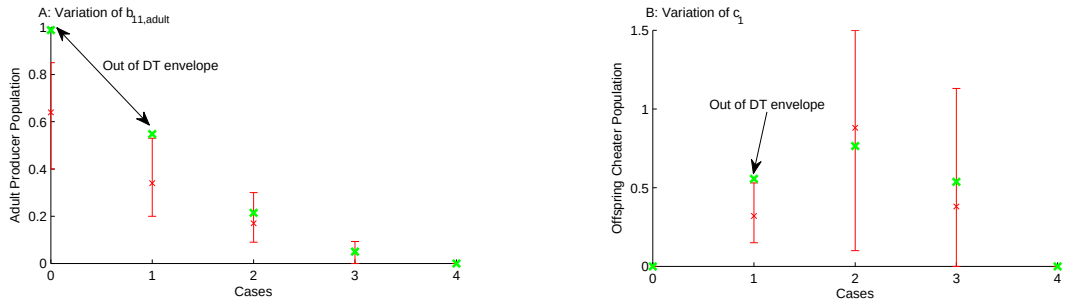

Figure 3.5: Sensitivity of the model to parameter variations. In red: maximum and minimum adult producer population (A) and cheater offspring population (B) after 64 days from Dobata and Tsuji. In green the model results after parameter variation (A) parameter $b_{11,adult}$ in 19%, (B) parameter c_1 in 9% showing model sensitivity.

Finally in an attempt to simplify the P^3G model using its sensitivity to the parameters the terms $b_{11,offs}, d_{12}, b_{2,adult}$ and d_{21} were suppressed generating a new model with 11 parameters instead of 15. [1]

With this simplification the new vector of parameters was optimized with the same procedure as used for the estimation, obtaining a new set of parameters shown in the table 3.4. The objective function value for the reduced set is $E(p_{reduced}) = 0,0881$ while the objective function value with all the parameters is $E(p_{all}) = 0,0898$ showing that removal of the parameters does not make significant difference to the error. It is also possible to confirm visually that the reduced model figure 3.6 presents a similar behavior to the model with all the parameters in figure 3.2.

[1] It should be observed that even when the model has large allowed variation to some parameters, such as the density population limiter d_{14}, the reproduction inhibition function $f(y)$, and starvation function $g(z)$, they cannot be eliminated, since they involve specific characteristics of the model

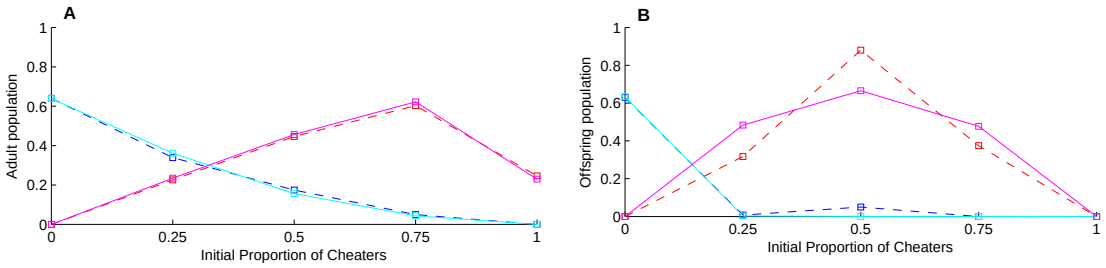

Figure 3.6: Comparision between the simulation results of reduced P^3G model and the experimental data for both species. A:Proportion of surviving adults, B: Offspring produced. Blue curve: workers experimental data, cyan curve: workers simulation results, red curve: Cheaters experimental data, pink curve: Cheaters simulation results.

3.3 Model with long term restocking

Now, with the parameters defined for the P^3G model in 2.31 and the simulation results accompanying the experiments of Dobata and Tsuji, we proceed to analyze the P^3G model in long term. From this section onwards, we return to the model 2.31 composed of three variables. We assume that the adult populations receive continuous restocking from the offspring by unifying $b_{i\ offs}$ and $b_{i\ adult}$ of each specie into one growth rate b_i.

The simulations in this section show the evolution of the five cases over the time. The curves of the five cases of each population and resource were plotted simultaneously, to monitor the evolution of the workers and the cheaters related to the level of the PGs in order to analyse the long term behavior.

In order to study long term behavior, we extended the simulation time to 360 days to observe specifically the initial conditions for which nests survive and for which they become extinct. The simulations for the P^3G model with restocking are shown in figure 3.7.

Parameters	Values	Parameters	Values
b_{11}	0.0136	c_1	1.8
b_{12}	0.0066	c_4	21
d_{11}	0	c_5	10
d_{12}	0.0305		
d_{14}	0.001	α_2	499.99
		α_3	3
b_{21}	0.0426		
d_{21}	0		
d_{22}	0.023	$*E(p)$	0.0881

Table 3.4: Estimated values for the reduced set of parameters in the P^3G model, and the objective function $E(p)$ calculated.

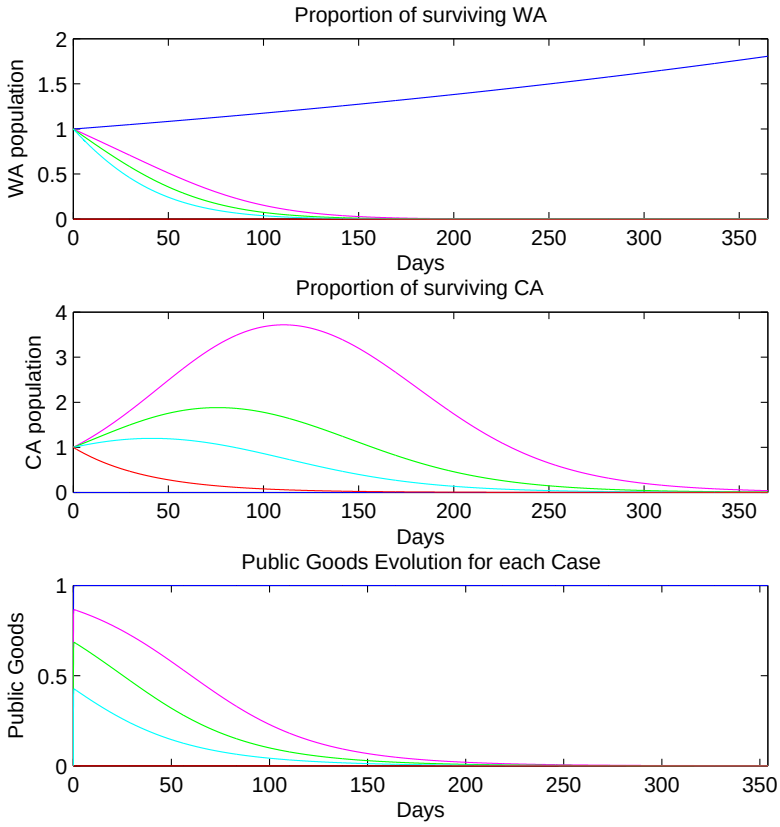

Figure 3.7: Simulation for the worker population, cheater population and Public Goods in five cases format. Blue: Case 0, Pink: Case 1, Green: Case 2, Cyan: Case 3 and Red: Case 4.

In the evolution of the P^3G model with restocking, two behaviors are noted immediately: one behavior in presence of cheaters and another in their absence.

With the existence of cheaters in the colony, initially, the cheater population grows, while the workers bear the weight of the non-productive cheater population. Eventually, the worker population is overtaken by the cheater population leading to a point where the PGs are consumed faster than they are produced. This means that the PGs production rate $\dot{z}$ becomes negative, which, in turn, means that a reduction in the stocks occurs until it reaches a level where the workers and the cheaters cannot be sustained and the system goes toward the extinction. In the context of the experiments, the low level of PGs represents the absence of worker ants taking care of the broods of both species as well as the hygiene in the nest.

This leads the extinction of the colony, due to the presence of cheaters, and occurs due to the high reproduction rate of the cheater population by one side and together with the drastic drop in reproduction rate of the workers. Recalling the model construction in the

section 2.2 the reproduction rate of the workers is limited by the existence of cheaters, which is modelled by the reproduction inhibition function $f(y)$ in (2.21).

Analysing the behavior of the reproduction rate of the workers, it is possible to observe from (2.21) and (2.31), that in absence of cheaters $y = 0$ which implies $f(y) = 1$, then the reproduction rate is influenced only by b_{12} (since $b_{11,offs} = 0$ from the estimation of the parameters, table 3.4). In contrast, with the presence of cheaters in the colony, $y > 0$, implying $f(y) \approx 0$, in this case the reproduction rate for the worker population becomes almost zero.

From table 3.1 it is plausible to conjecture that the cheaters have larger growth rate than the worker. Indeed, assuming $z = 1$,

$$\begin{aligned} \text{growth}_{worker} &= \left[(b_{11} + b_{12})c_4 - d_{11} - d_{12}\phi(z)\right], \\ \text{growth}_{cheater} &= \left[b_2 c_5 - d_{21}\right] \end{aligned} \tag{3.7}$$

and using the values of the table 3.4 in (3.7), we obtain:

$$\begin{aligned} \text{growth}_{worker} &= 0,4242 - d_{11}\phi(z), \\ \text{growth}_{cheater} &= 0.426 \\ \therefore\ \text{growth}_{cheater} &> \text{growth}_{worker} \end{aligned}$$

verifying our conjecture.

As explanation lets take the model (2.31) without the overcrowding term d_{14}, and analyze the possible behavior. In the absence of cheaters in the environment, the nest evolves and the worker population grows unbounded. The PGs grows reaching a maximum value and stabilizing even if the workers population grows indefinitely.

In absence of cheaters (case 0), analysed in section 2.3, the workers present an exponential growth behavior while the PGs stabilize at the value M. In order to arrive at a more realistic model, the overcrowding term d_{14} was used. The overcrowding term d_{14} makes the trajectories of the model display limited growth of the worker population (3.8).

As is possible to observe in figure 3.8, the value selected for d_{14} determines the growth limit in the workers dynamics. There are no data in the experiments of Dobata and Tsuji about the population density limits for the *P. punctatus* species. Thus an arbitrary value for the term was selected in order to demonstrate its functionality.

In order to observe the evolution of the proposal with the estimated parameters, the term d_{14} was chosen as 1×10^{-3} and the model was simulated. The results are shown in figure 3.9.

It is noticeable that the cheaters trajectories (cases 1, 2, 3 and 4), do not change

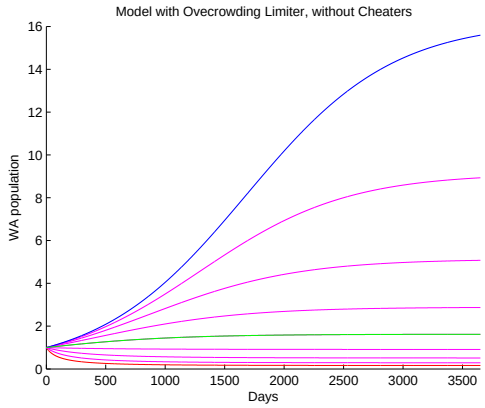

Figure 3.8: P^3G model with limiter in absence of cheaters, variation of the term d_{14}. Red curve $d_{14} = 1 \times 10^{-2}$, Green curve $d_{14} = 1 \times 10^{-3}$, Blue curve $d_{14} = 1 \times 10^{-4}$.

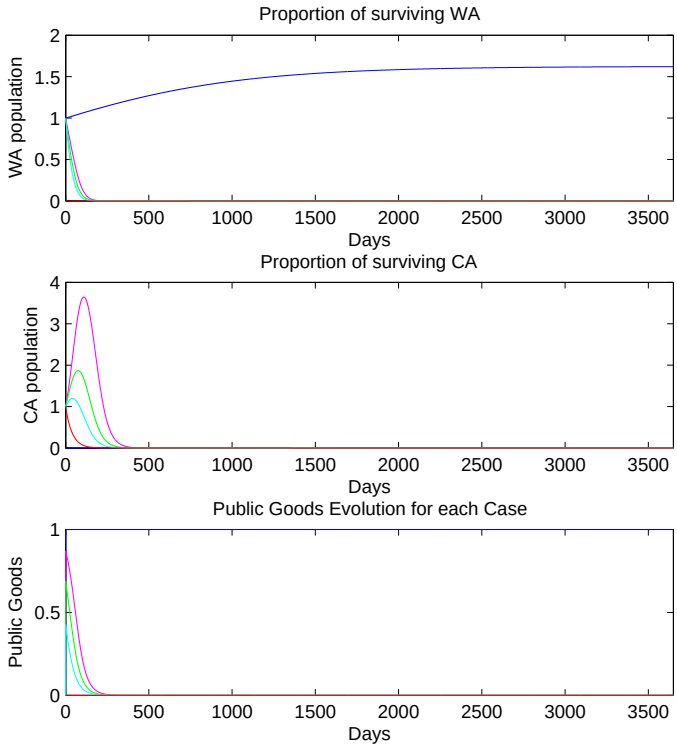

Figure 3.9: Simulations with $d_{14} = 0,001$ for the worker population, cheater population and Public Goods in five cases format. Blue: Case 0, Pink: Case 1, Green: Case 2, Cyan: Case 3 and Red: Case 4.

their behavior with the inclusion of the term d_{14}. In order to observe how the P^3G model reaches steady state induced by the limiter in the Case 0, the simulation time was extended to $t = [0, 3600]$.

Chapter 4

Algebraic Conditions for Positivity and Stability of the P^3G Model Equilibria

This chapter starts by calculating all equilibria of the proposed P^3G model. This is followed by an analysis to establish conditions for the positivity of the equilibria. Then, local stability of the equilibria is studied, by linearising the P^3G model. All calculations are symbolic, resulting in algebraic conditions. Finally these conditions are calculated numerically, using the parameters of the fitted P^3G model.

4.1 Formulas for the equilibrium points of the P^3G model

The equilibrium points of the P^3G model were determined from (2.31). Recall from chapter 2 that setting the term $d_{14} = 0$ causes the model trajectories to become unbounded, while imposing $d_{14} > 0$ ensures that the model trajectories remain bounded.

It is easy to determine the existence of an equilibrium point $P_0 = (0, 0, z_0)$ which represents the extinction of both species of ants, independent of the initial value of z. In order to determine other equilibrium points different from extinction, the cheaters equation from (2.31) is set to zero as the starting point for the analysis:

We denote the equilibrium point as $x^*,\ y^*,\ z^*$.

$$b_2 c_5 \rho_M z^* - (d_{21} + d_{22} g(z^*)) = 0 \tag{4.1}$$

Substituting the starvation function $g(z)$ from (2.33) into (4.1) we obtain:

$$\alpha_3 b_2 c_5 \rho_M z^{*2} + (b_2 c_5 \rho_M - \alpha_3 d_{21})\, z^* - (d_{21} + d_{22}) = 0 \tag{4.2}$$

From (4.2) the equilibria z_j^*, $j = 1, 2$, are:

$$z_j^* = \frac{-(b_2 c_5 \rho_M - \alpha_3 d_{21}) \pm \sqrt{(b_2 c_5 \rho_M - \alpha_3 d_{21})^2 + 4\alpha_3 b_2 c_5 \rho_M (d_{21} + d_{22})}}{2\alpha_3 b_2 c_5 \rho_M} \tag{4.3}$$

In this analysis our interest is focused on positive PGs, thus only on the positive equilibrium denoted as z_+^*. Defining g^* and φ^* as the results of substituting z_+^* into the starvation function $g(z)$ in (2.33) and into the working force $\varphi(z)$ in (2.34), we obtain:

$$g^* = g\left(z_+^*\right) = \frac{1}{1 + \alpha_3 z_+^*} \tag{4.4}$$

$$\varphi^* = \varphi\left(z_+^*\right) = 1 + g(z_+^*) \tag{4.5}$$

The next step is to find the PG equilibria. From (2.31), setting $\dot{z} = 0$.

$$c_1 \varphi^* \rho_M^{-1} x^* - c_4 x^* z_+^* - c_5 y^* z_+^* = 0 \tag{4.6}$$

From (4.6) we solve for y^* in terms of x^*:

$$y_i^* = \frac{1}{\alpha_2} e_1 x_i^* \tag{4.7}$$

where,

$$e_1 = \frac{\alpha_2 \left(c_1 \varphi^* - c_4 \rho_M z_+^*\right)}{c_5 \rho_M z_i^*} \tag{4.8}$$

Substituting y_i^* from (4.7) into the reproduction inhibition function $f(y)$ in (2.21), gives

$$f\left(y_i^*\right) = \frac{1}{1 + e_1 x_i^*} \tag{4.9}$$

In order to find the equilibrium for x, setting $\dot{x} = 0$ in (2.31).

$$\left(b_{11} + b_{12} f\left(y_i^*\right)\right) c_4 \rho_M z_+^* - \left(d_{11} + d_{12}\varphi\left(z_+^*\right) + d_{14} x^*\right) = 0 \tag{4.10}$$

Substituting $f(y_i^*)$ from (4.9) and after some algebra, we obtain:

$$\frac{b_{12} c_4 \rho_M z_+^*}{1 + e_1 x_i^*} - d_{14} x_i^* = e_2 \tag{4.11}$$

where,

$$e_2 = d_{11} + d_{12}\varphi^* - b_{11}c_4\rho_M z_+^* \tag{4.12}$$

Equation (4.11) can be rewritten as:

$$d_{14}e_1 x_i^{*2} + (d_{14} + e_1e_2)x_i^* + (e2 - b_{12}c_4\rho_M z_+^*) = 0 \tag{4.13}$$

From (4.13), the equilibrium values in x, assuming $d_{14} > 0$, are:

$$x_i^* = \frac{-(d_{14} + e_1e_2) \pm \sqrt{(d_{14} + e_1e_2)^2 + 4d_{14}e_1(b_{12}c_4\rho_M z_+^* - e_2)}}{2d_{14}e_1} \tag{4.14}$$

Thus possible positive equilibrium points other than extinction are: $P_i(x_i, y_i, z_+^*)$, where $i = 1, 2$.

4.2 Algebraic conditions for the positivity of the equilibrium points

The conditions to obtain positive equilibrium points are calculated under the assumption that all the parameters defining the P^3G model are positive. The analysis of the conditions is carried out using the same sequence as for the calculation of the equilibrium points, in other words, first z, then y, and finally x.

4.2.1 Positivity condition for the equilibrium in the Public Goods

The equilibrium in z^* in (4.3) can be written as:

$$z_j^* = \frac{-\beta_3 \pm \sqrt{\beta_3^2 + \Delta_3}}{2\alpha_3 b_2 c_5 \rho_M} \tag{4.15}$$

where,

$$\beta_3 = (b_2c_5\rho_M - \alpha_3 d_{21}) \tag{4.16}$$

$$\Delta_3 = 4\alpha_3 b_2 c_5 \rho_M (d_{21} + d_{22}) \tag{4.17}$$

From (4.15), positive z^* results if the following condition is met.

$$\sqrt{\beta_3^2 + \Delta_3} > \beta_3 \tag{4.18}$$

which is fulfilled if $\Delta_3 > 0$, i.e, from (4.17)

$$4\alpha_3 b_2 c_5 \rho_M (d_{21} + d_{22}) > 0 \tag{4.19}$$

which is clearly true if all the parameters in (4.19) are positive.

Then we conclude always exist a positive and a negative equilibrium for z^*. Given that the PGs are positive values, from now on z^* represents the positive equilibrium in z.

4.2.2 Positivity condition for the equilibrium in cheater ant population

Since all equilibrium points are positive, then $x^* > 0$ and $z^* > 0$. Given the equilibrium in (4.7), y^* is positive if:

$$e_1 > 0 \tag{4.20}$$

From (4.8), (4.20) is satisfied if:

$$\frac{c_1}{c_4 \rho_M} - \frac{z_+^*}{\varphi^*} > 0 \tag{4.21}$$

4.2.3 Positivity conditions for the equilibrium in worker ant population

Assuming (4.20) is satisfied, conditions for a positive equilibrium value in x for the P^3G model in (2.31) to exist, are derived as follows.
Equation (4.14) is written as:

$$x_i^* = \frac{-\beta_1 \pm \sqrt{\beta_1^2 + \Delta_1}}{2 d_{14} e_1} \tag{4.22}$$

where,

$$\beta_1 = d_{14} + e_1 e_2 \tag{4.23}$$

$$\Delta_1 = 4 d_{14} e_1 \left(b_{12} c_4 \rho_M z_+^* - e_2 \right) \tag{4.24}$$

Thus the conditions to achieve a positive value in x^* are divided into two cases:

- **Case 1:**

$$\sqrt{\beta_1^2 + \Delta_1} > \beta_1 \tag{4.25}$$

(4.25) is fulfilled if $\Delta_1 > 0$, then $\left(b_{12} c_4 \rho_M z_+^* - e_2 \right) > 0$, and we find, after some

algebra, that x^* is positive if:

$$b_{11} + b_{12} - \frac{d_{11} + d_{12}\varphi^*}{c_4 \rho_M z_+^*} > 0 \tag{4.26}$$

- **Case 2:**

$$\sqrt{\beta_1^2 + \Delta_1} < \beta_1 \text{ and } \beta_1 < 0 \tag{4.27}$$

(4.27) is fulfilled if:

$$b_{12} c_4 \rho_M z_+^* - e_2 < 0 \tag{4.28}$$

$$d_{14} + e_1 e_2 < 0 \tag{4.29}$$

Finally this conditions are true depending on the values taken by the parameters, which will be analysed in section 4.5.

4.3 Local stability conditions for the P^3G model

In order to analyze local stability in the vicinity of the equilibrium points, the Jacobian of the P^3G model is calculated from (2.31).

Denote the Jacobian matrix evaluated at the equilibrium points as J_k, for $k = 1, 2$.

$$J_k = J(P_k) = \begin{bmatrix} J_{11} & J_{12} & J_{13} \\ J_{21} & J_{22} & J_{23} \\ J_{31} & J_{32} & J_{33} \end{bmatrix}_{P_k} \tag{4.30}$$

where, J_{lm} are the partial derivatives of the model evaluated at the equilibrium point, and are presented in Appendix D .

The characteristic polynomial of the Jacobian was calculated first in order to use the Routh-Hurwitz stability criterion to determine local stability around the equilibrium point.

The characteristic equation of the Jacobian is given by:

$$Det\,(J - \lambda I) = \lambda^3 - Tr(J)\lambda^2 - \frac{1}{2}(J_{ij}J_{ji} - J_{ii}J_{jj})\lambda - Det(J) = 0 \tag{4.31}$$

which is denoted:

$$\lambda^3 + s_2\lambda^2 + s_1\lambda + s_0 = 0 \tag{4.32}$$

so that,

$$s_2 = -Tr(J) = -(J_{11} + J_{22} + J_{33})$$
$$s_1 = \frac{1}{2}(J_{22}J_{33} - J_{23}J_{32} + J_{33}J_{11} - J_{31}J_{13} + J_{11}J_{22} - J_{12}J_{21})$$
$$s_0 = -Det(J) = -J_{11}J_{22}J_{33} - J_{12}J_{23}J_{31} - J_{13}J_{21}J_{32} + J_{31}J_{22}J_{13} + J_{21}J_{12}J_{33} + J_{11}J_{23}J_{32}$$

From Routh-Hurtwitz criterion, the polynomial (4.32) is stable if the following conditions are true:

$$s_2 > 0 \tag{4.33}$$
$$s_1 > 0 \tag{4.34}$$
$$s_0 > 0 \tag{4.35}$$
$$s_2 s_1 - s_0 > 0 \tag{4.36}$$

4.3.1 Stability analysis for the origin

The remaining equilibrium point to analyze is the origin $P_0 = (0, 0, z_0)$. Evaluating the Jacobian in (4.30) at $(0, 0, z_0)$, we obtain the following characteristic equation:

$$\lambda^3 - (J_{11} + J_{22})\lambda^2 + J_{11}J_{22}\lambda = 0 \tag{4.37}$$

The eigenvalues of (4.37) are:

$$\lambda_1 = J_{11} = (b_{11} + b_{12})c_4\rho_M z - (d_{11} + d_{12}\varphi(z)) \tag{4.38}$$
$$\lambda_2 = J_{22} = b_2 c_5 \rho_M z - (d_{21} + d_{22}g(z)) \tag{4.39}$$
$$\lambda_3 = 0 \tag{4.40}$$

We now determine positive values of z for which P_0 is stable. The roots of (4.38) and (4.39) are found by setting $\lambda_1 = 0$ and $\lambda_2 = 0$ and with some algebra we obtain:

$$z_{\lambda_1} = \frac{-\gamma_1 + \sqrt{\gamma_1^2 + 4\alpha_3(b_{11} + b_{12})c_4\rho_M(d_{11} + 2d_{12})}}{2\alpha_3(b_{11} + b_{12})c_4\rho_M} \tag{4.41}$$

$$z_{\lambda_2} = \frac{-\gamma_2 + \sqrt{\gamma_2^2 + 4\alpha_3 b_2 c_5 \rho_M(d_{21} + d_{22})}}{2\alpha_3 b_2 c_5 \rho_M} \tag{4.42}$$

where

$$\gamma_1 = ((b_{11} + b_{12})c_4\rho_M - \alpha_3(d_{11} + d_{12}))$$
$$\gamma_2 = (b_2c_5\rho_M - \alpha_3 d_{21})$$

Knowing the values of z_{λ_1} and z_{λ_2} it is possible to analyze the behavior of the origin with respect the value of z, through the following case:

- **Case 1** $z = 0$**:**

  The origin is attractive because the eigenvalues are nonpositives, since in this case:

$$\begin{cases} \lambda_1 &= -(d_{11} + 2d_{12}) \\ \lambda_2 &= -(d_{21} + d_{22}) \\ \lambda_3 &= 0 \end{cases} \tag{4.43}$$

- **Case 2** $z < z_{1\lambda_2} < z_{1\lambda_1}$**:**

  The origin is attractive because, since in this case:

$$\begin{cases} \lambda_1 &< 0 \\ \lambda_2 &< 0 \\ \lambda_3 &= 0 \end{cases} \tag{4.44}$$

- **Case 3** $z_{1\lambda_2} < z_{1\lambda_1} < z$**:**

  The origin is unstable and repulsive in two axes because:

$$\begin{cases} \lambda_1 &> 0 \\ \lambda_2 &> 0 \\ \lambda_3 &= 0 \end{cases} \tag{4.45}$$

For the other cases $z_{1\lambda_2} < z < z_{1\lambda_1}$ and $z_{1\lambda_1} < z < z_{1\lambda_2}$, the origin is unstable.

4.4 Local stability analysis for the P^3G model in absence of cheaters

The first part of the stability analysis, is carried out assuming the absence of cheater ants, in order to describe the nest development in absence of the invasive cehaters. The

inverse situation, absence of workers, as seen above, leads to the extinction of cheaters, given that the PGs are only produced by the worker population.

The P^3G model in (2.31) without cheaters has: $y(0) = 0$ and $\dot{y} = 0$, $f(y) = 1$, i.e.:

$$\begin{aligned} \dot{x}_{nc} &= \left[(b_{11} + b_{12})\, c_4 \rho_M z_{nc} - (d_{11} + d_{12}\varphi(z_{nc}) + d_{14} x_{nc})\right] x_{nc} \\ \dot{z}_{nc} &= \left[c_1 \varphi(z_{nc}) \rho_M^{-1} - c_4 z_{nc}\right] x_{nc} \end{aligned} \tag{4.46}$$

where x_{nc} and z_{nc} are the variables of the model in absence of the cheater population.

From (4.46) it is possible to determine an equilibrium point $(0, 0, z_{nc})$, which correspond to the extinction of the workers, independent of the initial PG value.

4.4.1 Equilibrium for public goods in the absence of cheaters

Equilibrium points other than the extinction are obtained by setting $\dot{z}_{nc} = 0$:

$$\begin{aligned} & c_1 \varphi(z_{nc}) \rho_M^{-1} - c_4 z_{nc} = 0 \\ & \alpha_3 c_4 \rho_M z_{nc}^{*2} + (c_4 \rho_M - \alpha_3 c_1) z_{nc}^{*} - 2c_1 = 0 \end{aligned}$$

Thus the possible equilibrium values for z_{nc} are:

$$\frac{-(c_4 \rho_M - \alpha_3 c_1) \pm \sqrt{(c_4 \rho_M - \alpha_3 c_1)^2 + 8\alpha_3 c_4 \rho_M c_1}}{2\alpha_3 c_4 \rho_M} \tag{4.47}$$

Choosing the positive value of the square root to define z_{nc}^{*}, using (2.35) and after some algebra:

$$z_{nc}^{*} = \frac{1}{M} \left[\frac{-(c_2 - \alpha_3 c_1) + \sqrt{(c_2 - \alpha_3 c_1)^2 + 8\alpha_3 c_2 c_1}}{2\alpha_3 c_1} \right] \tag{4.48}$$

The expression inside the brackets in (4.48) is identical to M (defined in (2.27)), which implies that the positive equilibrium in z_{nc}^{*} for the P^3G model without cheaters is:

$$z_{nc}^{*} = 1 \tag{4.49}$$

4.4.2 Equilibrium for the workers in the absence of cheaters

The equilibrium for the worker ants equation was found by setting $\dot{x}_{nc} = 0$, and from (4.46), this implies that:

$$(b_{11} + b_{12}) c_4 \rho_M z_{nc} - (d_{11} + d_{12}\varphi(z_{nc}) + d_{14} x_{nc}) = 0 \tag{4.50}$$

From (4.50) the equilibrium value in x_{nc} can be found by replacing $z_{nc}^{*} = 1$, into (4.50)

to get:

$$x_{nc}^{*} = \frac{1}{d_{14}} \left[(b_{11} + b_{12})\, c_4 \rho_M - \left(d_{11} + d_{12} \left(1 + \frac{1}{1+\alpha_3} \right) \right) \right] \tag{4.51}$$

From (4.51), the condition to achieve positive population in x_{nc} is given by:

$$b_{11} + b_{12} > \frac{d_{11} + d_{12} \left(1 + \frac{1}{1+\alpha_3} \right)}{c_4 \rho_M} \tag{4.52}$$

4.4.3 Stability analysis in the absence of cheaters

In order to determine the stability of the P^3G model in 2.31, in absence of cheaters, the Jacobian was recalculated, yielding:

$$J_{nc} = J\left(x_{nc}^{*}, 0, z_{nc}^{*}\right) = \begin{bmatrix} J_{11} & J_{13} \\ J_{31} & J_{33} \end{bmatrix} \tag{4.53}$$

Calculating the partial derivatives in (4.53), we obtain:

$$J_{11}(x_{nc}^{*}, 0, 1) = (b_{11} + b_{12}) c_4 \rho_M - \left[d_{11} + d_{12} \left(1 + \frac{1}{1+\alpha_3} \right) + 2 d_{14} x_{nc}^{*} \right]; \tag{4.54}$$

$$J_{13}(x_{nc}^{*}, 0, 1) = \left[(b_{11} + b_{12}) c_4 \rho_M + \frac{\alpha_3 d_{12}}{(1+\alpha_3)^2} \right] x_{nc}^{*}; \tag{4.55}$$

$$J_{31}(x_{nc}^{*}, 0, 1) = c_1 \rho_M^{-1} \left(1 + \frac{1}{1+\alpha_3} \right) - c_4; \tag{4.56}$$

$$J_{33}(x_{nc}^{*}, 0, 1) = -\left[\frac{\alpha_3 c_1 \rho_M^{-1}}{(1+\alpha_3)^2} + c_4 \right] x_{nc}^{*}; \tag{4.57}$$

substituting (4.51) into (4.54) yields,

$$J_{11}(x_{nc}^{*}, 0, 1) = -\left[(b_{11} + b_{12}) c_4 \rho_M - \left(d_{11} + d_{12} \left(1 + \frac{1}{1+\alpha_3} \right) \right) \right] \tag{4.58}$$

Assuming the model in (4.46) in presence of the maximum production of PGs ($z^{*} = 1$), presents a behavior of growing population, then the value inside the brackets of (4.58) should be positive and the component J_{31} in (4.56) should be positive too, given that, with $z^{*} = 1$, the PGs at least should present a production rate greater than or equal to the consumption rate.

Then, assuming the equilibrium point $x_{nc}^{*} > 0$ for the Jacobian the following notation

is introduced:

$$\begin{aligned} J_{11}(x^*_{nc}, 0, 1) &= -j_a \\ J_{13}(x^*_{nc}, 0, 1) &= j_b x^*_{nc} \\ J_{31}(x^*_{nc}, 0, 1) &= j_c \\ J_{33}(x^*_{nc}, 0, 1) &= -j_d x^*_{nc} \end{aligned} \tag{4.59}$$

where,

$$\begin{aligned} j_a &= (b_{11} + b_{12})c_4\rho_M - \left(d_{11} + d_{12}\left(1 + \frac{1}{1+\alpha_3}\right)\right) > 0; \\ j_b &= (b_{11} + b_{12})c_4\rho_M + \frac{\alpha_3 w d_{12}}{(1+\alpha_3)^2} > 0; \\ j_c &= c_1\rho_M^{-1}\left(1 + \frac{1}{1+\alpha_3}\right) - c_4 > 0; \\ j_d &= \frac{\alpha_3 w c_1 \rho_M^{-1}}{(1+\alpha_3)^2} + c_4 > 0; \end{aligned}$$

Using (4.59) of the characteristic equation the Jacobian in (4.53) is:

$$\lambda^2 + (j_a + j_d x^*_{nc})\lambda + j_a j_d x^*_{nc} - j_b j_c x^*_{nc} \tag{4.60}$$

so that its eigenvalues are:

$$\lambda_{i,nc} = \frac{-(j_a + j_d x^*_{nc}) \pm \sqrt{(j_a + j_d x^*_{nc})^2 - 4(j_a j_d x^*_{nc} - j_b j_c x^*_{nc})}}{2} \tag{4.61}$$

From (4.61), both eigenvalues are negative if

$$(j_a j_d x^*_{nc} - j_b j_c x^*_{nc}) = Det(J_{nc}) > 0$$

which implies

$$(j_a + j_d x^*_{nc}) > \sqrt{(j_a + j_d x^*_{nc})^2 - 4Det(J_{nc})}$$

From (4.61), factoring the values inside the square root, we obtain:

$$\lambda_{i,nc} = \frac{-(j_a + j_d x^*_{nc}) \pm \sqrt{(j_a - j_d x^*_{nc})^2 + 4 j_b j_c x^*_{nc}}}{2} \tag{4.62}$$

From (4.62) it follows that the eigenvalues are real, and if $Det(J_{nc}) > 0$ the eigenvalues are real and negative.

Thus the conditions to achieve a stable positive equlibrium point in absence of

cheaters, are given by:

$$j_a > 0; \tag{4.63}$$

$$j_c > 0; \tag{4.64}$$

$$Det(J_{nc}) > 0; \tag{4.65}$$

4.5 Application of the conditions to the fitted P^3G model

The equilibrium points for the fitted P^3G model in (2.31) are analysed for the positive conditions.

From condition 4.19, there always exists a positive value for z^*.

Positivity for y^* is given by the condition in (4.20) when the condition (4.21) is true. Calculating z^* from (4.3), and substituting the parameters of table 3.1 into condition (4.21), we obtain:

$$\frac{c_1}{c_4\rho_M} - \frac{z^*}{\varphi^*} = 0,812$$

and condition (4.21) is satisfied. From (4.7) the values of y_i^* are positive if the values of x_i^* are positive too. Then, x^* is positive if one of the two cases in section 4.2.3 holds:

Case 1 does not holds because condition (4.26) is violated.

$$b_{11} + b_{12} - \frac{d_{11} + d_{12}\varphi_i}{c_4\rho_M z_i^*} = -0,0910, \quad \text{(should be positive)}$$

Case 2 also does not hold because condition (4.28) is violated.

$$b_{12}c_4\rho_M z_i^* - e_2 = -0,0303, \quad \text{(should be positive)}$$

Note, for the fitted P^3G model (model in (2.31) with the estimated parameters in table 3.1), even when the conditions to obtain positive z^* and y^* are true, the condition for positive x^* fails so that, there is no equilibrium point in the first octant.

Finally the values calculated for the equilibrium values x_i^*, y_i^* and z^* respectively in (4.14), (4.7) and (4.3) are shown in the table 4.5, confirming the previous analysis performed, namely, that they are all infeasible (at least one component is negative).

Equilibrium Point	x^*	y^*	z^*
P_1	-1.7×10^{-4}	-1.92×10^{-3}	1.79×10^{-1}
P_2	-3.17×10^{1}	-3.55×10^{2}	1.79×10^{-1}

Table 4.1: Summary of the equilibrium points for the P^3G model.

Stability of the origin with the fitted P^3G model

Replacing the estimated parameters in the table 3.1 into (4.41) and (4.42) we obtain the values for which eigenvalues of (4.37) becomes zero, by:

$$z_{\lambda_1} = 0.9555 \tag{4.66}$$

$$z_{\lambda_2} = 0.1790 \tag{4.67}$$

With this values we conclude from case 2 in (4.44) and case 3 in (4.45), respectively the origin is attractive for values in z less than 0,1790 and is repulsive for values higher than 0.9555.

4.5.1 Stability Results in Absence of Cheater Ants

In order to confirm if the estimated parameters allow stability in the model in absence of cheater ants, were calculated the conditions 4.63, 4.64 and 4.65 from the section 4.4.3, as follows:

$$j_a = (b_{11} + b_{12})c_4\rho_M - \left(d_{11} + d_{12}\left(1 + \frac{1}{1+\alpha_3}\right)\right) = 0.0016 \;\rightarrow\; j_a > 0$$

$$j_c = c_1\rho_M^{-1}\left(1 + \frac{1}{1+\alpha_3}\right) - c_4 = 21.7066 \;\rightarrow\; j_c > 0;$$

$$Det(J_{nc}) = 0.0571 \;\rightarrow\; Det(J_{nc}) > 0$$

Clearly from section 4.4.3, the P^3G model is stable if x^*_{nc} is positive, for that was calculated the equilibrium point P_{nc} from (4.51) and their respective eigenvalues in (4.61), and the results are as follows:

$$x^*_{nc} = \frac{1}{d_{14}}\left[(b_{11} + b_{12})\, c_4\rho_M - \left(d_{11} + d_{12}\left(1 + \frac{1}{1+\alpha_3}\right)\right)\right] = 1.6228 \tag{4.68}$$

Then, the eigenvalues are:

$$\lambda_{1,nc} = -0.0016$$

$$\lambda_{2,nc} = -35.2268$$

The eigenvalues for the model with no cheaters are negative, indicating the model is stable. Even more, is possible to confirm the origin becomes a repulsive equilibrium given the value of z_{nc} fixes in 1, which is higher than $z_{\lambda_1} = 0,9955$ making the $P_{0,nc}$ unstable. Then, the model in absence of cheaters is stable as is confirmed by the simulations in the section 3.3 for Case 0.

Chapter 5

Seeking Coexistence in the P^3G Model

As shown in section 4.5, the inevitable outcome in the fitted P^3G model with presence of cheaters is extinction. In this Chapter, we will use the conditions of Chap. 4 to carry out a parameter sweep in order to find parameter values for which the positivity and stability conditions are satisfied and then check through simulations if these parameter values do indeed lead to coexistence of workers and cheaters in the P^3G model. The intuitive reasoning behind the parameter sweep proposed to find coexistence goes as follows:

1. Extinction should no longer be a stable equilibrium point for the P^3G model.

2. From the experimental data to which the P^3G model was fitted, it is clear that the growth rate of workers in the presence of cheaters becomes too low to sustain the colony. Therefore increasing the worker growth rate parameter (b_{11}) is one possibility.

3. The experimental data also make it clear that cheater survival rate is very high. In other words, the death rates for cheaters (d_{21} and d_{22}) are too low, and thus they are also candidates for adjustment.

5.1 Local stability in the vicinity of the equilibrium points

In order to know which stability conditions are satisfied during the parameter sweep, a subroutine in Madonna software [30] was constructed. Since these parameters are growth or death rates the sweep is assumed to be between 0 and 1.

In order to determine the positivity in the equilibrium points and the stability in their vicinity, it is necessary to evaluate the following:

- The equilibrium points: x_i^*, y_i^* and z^*,
- The conditions in (4.33), (4.34) and (4.35) for stability, confirming positivity of the terms s_2, s_1 and s_0 of the polynomial,
- The condition in (4.36) for stability, confirming the stability criterion of Routh-Hurtwitz, by the expression $s_2 s_1 - s_0 > 0$.

These conditions are referred to in the subsequent analysis as positivity condition (for positive equilibrium points) and the stability condition.

Additionally, there is another condition of our interest that helps in finding a stable equilibrium. The condition $z^* > z_{1\lambda_1}$ described in section 4.3.1, defines the attractive or repulsive behavior of the origin. Thus the three conditions are defined as follows:

$$\text{Positivity Condition} = \begin{cases} True, & \text{if } x_i^* > 0,\ y_i^* > 0,\ z^* > 0 \\ False, & \text{otherwise.} \end{cases} \tag{5.1}$$

$$\text{Stability Condition} = \begin{cases} True & \text{if } s_2 > 0,\ s_1 > 0,\ s_0 > 0,\ s_2 s_1 - s_0 > 0 \\ False, & \text{otherwise.} \end{cases} \tag{5.2}$$

$$\text{Origin Stability} = \begin{cases} Repulsive, & \text{if } z^* > z_{1\lambda_1} \\ Attractive, & \text{otherwise.} \end{cases} \tag{5.3}$$

Based on these conditions, each parameter was varied over the interval [0,1] seeking simultaneous fulfillment of the three conditions (5.1) - (5.3). Figures 5.1 and 5.2 show the evolution of the satisfaction of the conditions for the equilibrium points P_1 and P_2, during the sweep of the parameters b_{11}, d_{21} and d_{22}.

- Sweep of parameter b_{11}: For values $b_{11} \geq 0,115$, the equilibrium point is positive but unstable. The stability condition as well as the positivity condition are true only for values greater than $b_{11} = 0,39$. However, the origin is still locally attractive since the origin stability condition in 5.3 is false over all the sweep.
- In the sweep of parameter d_{21}, P_2 is negative and unstable for the whole range scanned. For P_1, with the value of $d_{21} \geqslant 0,025$, the third condition is true implying $z_1^* > z_{1\lambda_1}$ which makes the origin unstable. Additionally, for a very short range between $0,02595 \leqslant d_{21} \leqslant 0,02609$, the positivity and stability conditions are true. There is another interval between $0,032 \leqslant d_{21} \leqslant 0,033$, where the positivity condition is true but P_1 is unstable.

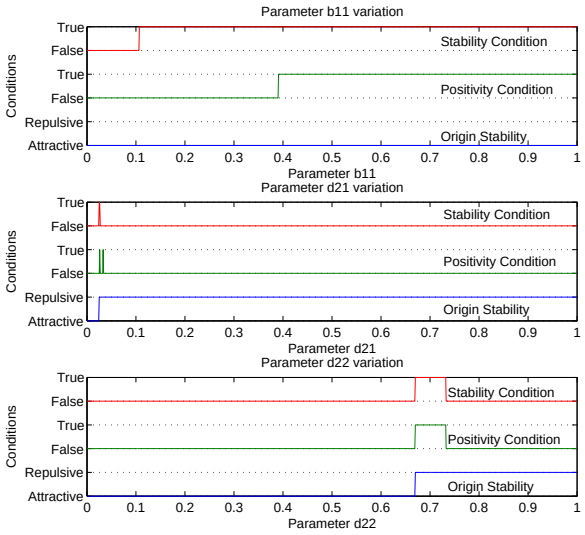

Figure 5.1: Stability conditions variation for P_1 with sweep of one parameter. Variation for : b_{11} (upper), d_{21} (middle) and d_{22} (bottom). Red curve stability condition, green curve positivity condition and blue curve origin stability.

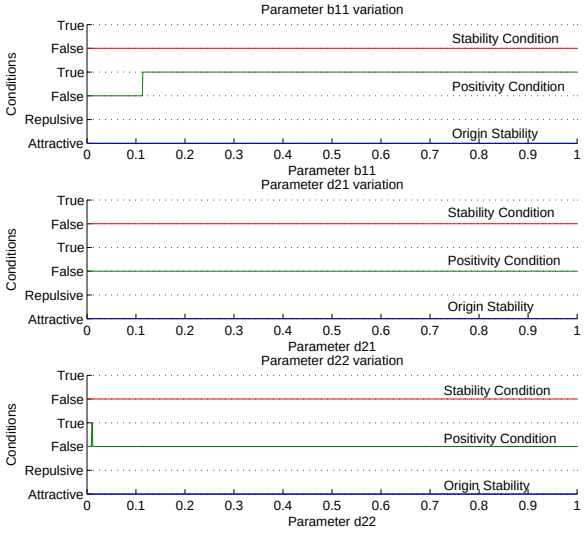

Figure 5.2: Stability conditions variation for P_2 with sweep of one parameter. Variation for : b_{11} (upper), d_{21} (middle) and d_{22} (bottom). Red curve stability condition, green curve positivity condition and blue curve origin stability.

- Sweep of d_{22}: similar to the previous sweep, P_2 is unstable and negative for almost all the variation, with an exception in the proximity of the point $d_{22} = 0,011$, where the equilibrium is positive, but unstable. For P_1, the condition (5.3) is true for the values of $d_{22} \geq 0,670$ and (5.1) and (5.2) are true too for the range $0,670 \leqslant d_{22} \leqslant 0,732$.

In conclusion, feasible parameter ranges for coexistence are $d_{21} \in [0,0259; 0,0260]$ or $d_{22} \in [0,670; 0,732]$, however, the values for the term d_{22} are too high compared with the estimated parameters in table 3.1, making these choices possibly unrealistic. The value $d_{21} = 0,026$ was chosen as the best option, because this value is similar to value of the fitted d_{22} (see table 3.1).

By setting $d_{21} = 0.026$ the survivor rate of the cheaters takes a plausible value, allowing the possibility of stability. The problem lies that this value the model is sensitive and any perturbation makes the equilibrium points become unstable. In order to solve this issue, the parameter b_{11} is swept again with $d_{21} = 0.026$ fixed, the figure 5.3 shows the results of the new sweep.

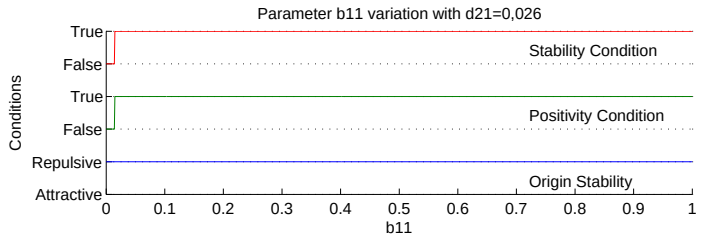

Figure 5.3: Stability conditions for P_1 setting $d_{21} = 0,026$ and sweeping the parameter b_{11}. Red curve stability condition, green curve positivity condition and blue curve origin stability.

Figure 5.3 shows P_1 is stable and positive for the values $b_{11} \geq 0,015$, where 0,015 is the current estimated value for the fitted P^3G model. Calculating the eigenvalues of the polynomial for P_1 with $b_{11} = 0,015$ and $d_{21} = 0,026$, gives:

$$\lambda_1 = -1,475,$$
$$\lambda_2 = -0,0001 + 0,0004i,$$
$$\lambda_3 = -0,0001 - 0,0004i.$$

This leads to lightly damped oscillatory behavior in the vicinity of P_1, as shown in figure 5.4, which shows the response to a perturbation of 10% in the initial condition P_1.

In order to improve the behavior of the fitted P^3G model a new value for b_{11} is chosen. Based on the sweep results in figure 5.3, we can increase b_{11} by 25% of its current value, maintaining the system stable, so, we set $b_{11} = 0.01875$. The simulation with the new parameters with a perturbation of 10% in the initial conditions is shown in figure 5.5.

As seen in figure 5.5, the system remains stable with the increase of the parameter b_{11}. In addition the oscillatory behavior vanishes, as can be expected on computing the

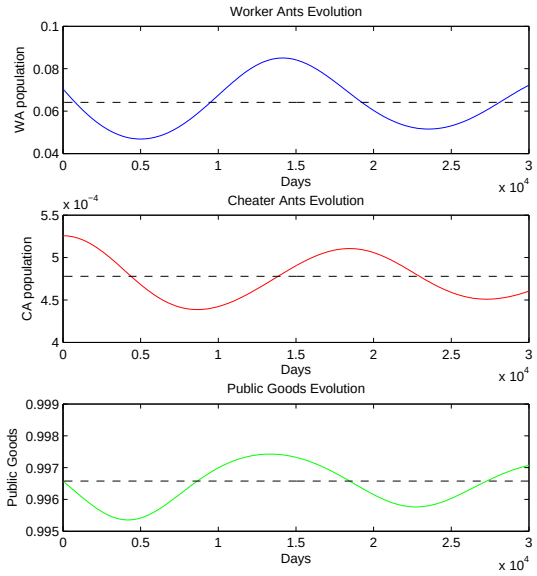

Figure 5.4: Evolution of the P^3G model with $d_{21} = 0,026$. Blue (upper): worker population curve, Red (middle) cheater population curve, Green (bottom) public goods curve, Black for the three variables denotes the equilibrium value of P_1.

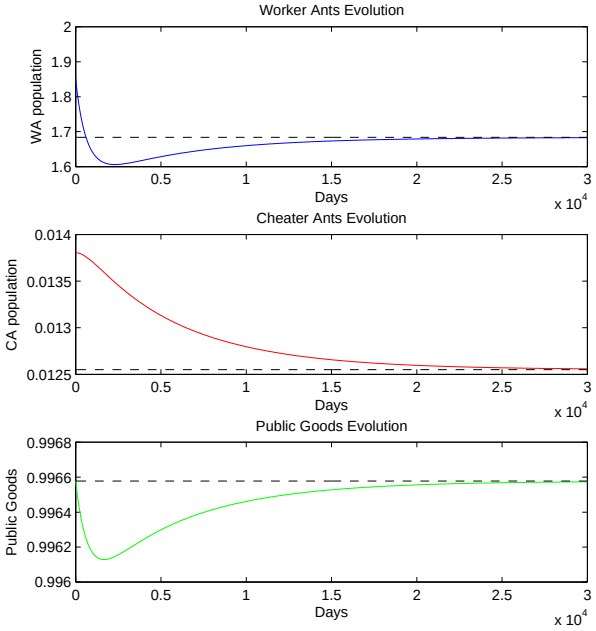

Figure 5.5: Dynamics of the fitted P^3G model with new parameters, $d_{21} = 0,026$ and $b_{11} = 0.01875$ in the vicinity of P_1. Blue (upper): worker population curve, Red (middle) cheater population curve, Green (bottom) public goods curve, Black for the three variables denotes the equilibrium value of P_1.

eigenvalues, which are all real and negative.

$$\lambda_1 = -36,6789,$$
$$\lambda_2 = -0,0015,$$
$$\lambda_3 = -0,0002.$$

The fitted P^3G model with the new values in the five cases format was simulated, in order to determine the behavior of the model with different initial populations, and the simulation obtained from this experiment is shown in figure 5.6.

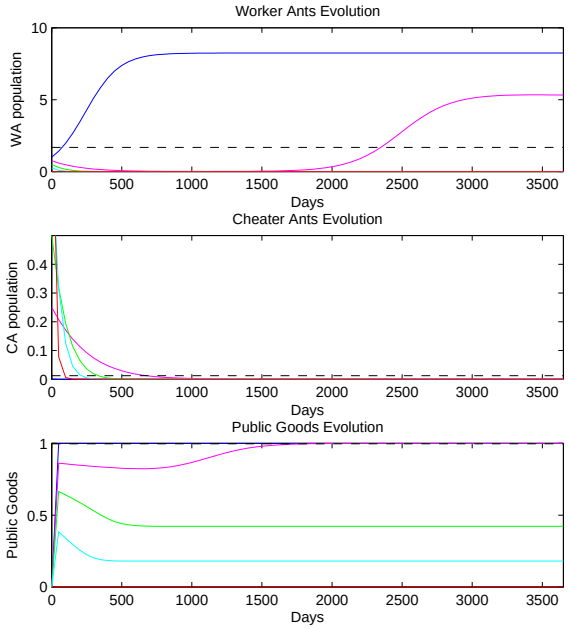

Figure 5.6: Dynamics of the fitted P^3G model with new parameter values $d_{21} = 0,026$ and $b_{11} = 0,01875$ in five cases format. Blue: Case 0, Pink: Case 1, Green: Case 2, Cyan: Case 3, Red: Case 4, Black: equilibrium values of P_1.

In figure 5.6, the only case different from extinction, is the case 0 (blue curve) with no cheaters and the case 1 (pink curve). For the rest of cases the colonies become extinct. For the case 1, the worker ants decrease their numbers until the cheaters are totally extinguished, in the moment the cheaters disappear, the case 1 becomes in a colony without cheaters being similar to the case 0. Note that the quantity of PG produced for the cases with cheaters does not reach the necessary value of $z^*_{\lambda_1}$ (for more information see section 4.3.1), which, in turn, maintains the origin attractive, leading the colonies to the extinction.

5.2 Achieving coexistence by modifying two parameters at a time

As noted in the previous section, to achieve stability in the five cases it was perceived that an increment in b_{11} is necessary. Based on the results of figure 5.3, the parameter b_{11} can be increased, while maintaining stability. Choosing it to be the double of its original value ($b_{11} = 0.03$) and simulating we obtain the results in figure 5.7.

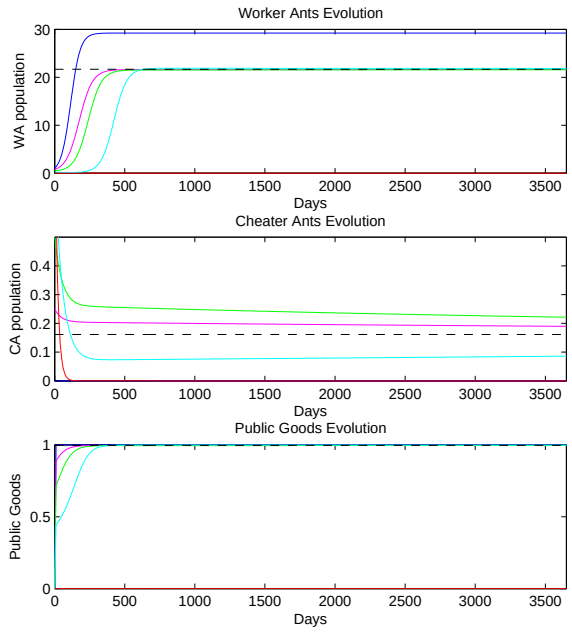

Figure 5.7: Dynamics of the fitted P^3G model with new parameters values $d_{21} = 0,026$ and $b_{11} = 0,03$ in five cases format. Blue: Case 0, Pink: Case 1, Green: Case 2, Cyan: Case 3, Red: Case 4, Black: equilibrium values of P_1.

As observed in figure 5.7, with the choices of the parameters as $d_{21} = 0.026$ and $b_{11} = 0.03$, coexistence emerges between the two populations. As expected, the only colony that becomes extinct is the one composed of only cheaters.

Interpretation of the values to achieve coexistence

One of the possibilities to achieve coexistence for this experimental colonies is by achieving the following two conditions:

- Doubling the current growth rate of the worker ants, which implies doubling both the brood production and the rate of maintenance of the adult population. This can also be interpreted as follows: if the current growth rate of the workers is kept

fixed, then is required to triple the reproduction rate of the broods in order to achieve the growth rate of $b_{11} = 0,03$.

- Changing the value of the death rate by age (d_{21}) of the cheater ants to a similar value of the death rate by starvation (d_{22}). This means both the death rates by age and by starvation have similar values, which decreases the survival rate of the cheaters.

5.3 Achieving coexistence by reducing the influence of the cheaters on the workers' reproduction rate

In this section we assume that the worker population can not reach the value proposed for $b_{11} = 0.03$. And we consider another alternative to achieve coexistence.

Observe that the reproduction rate of the workers in 2.31, is dependent on the existence of cheaters in the nest. This dependence (in the growth term for the workers) impedes the possibility of coexistence of the two species.

In order to achieve coexistence between the populations, we return to the values of the parameters selected in section 5.1, which are $d_{21} = 0.026$ and $b_{11} = 0.01875$, and remove the influence of the cheaters on the growth rate of the workers, by setting $\alpha_2 = 0$ (which implies $f(y) = 1$ and $(b_{11} + b_{12}) = b_1$). Thus we obtain the model of the worker population uninfluenced by the cheaters as follows:

$$\begin{aligned} \dot{x}_{wu} &= \left[(b_1 c_4 \rho_M z_{wd} - (d_{11} + d_{12}\varphi(z_{wu}) + d_{14} x_{wu})\right] x_{wu} \\ \dot{y}_{wu} &= \left[b_2 c_5 \rho_M z_{wu} - (d_{21} + d_{22} g(z_{wu}))\right] y_{wu} \\ \dot{z}_{wu} &= c_1 \varphi(z_{wu}) \rho_M^{-1} x_{wu} - (c_4 x_{wu} + c_5 y_{wu})\, z_{wu} \end{aligned} \tag{5.4}$$

where, x_{wu} and z_{wu} respectively are the worker population uninfluenced by the cheaters and the PGs. The equilibrium points of (5.4) are calculated in the Appendix E.

The dynamics of the "uninfluenced" model in (5.4) with the estimated parameters in table 3.1 and choice of the parameters $d_{21} = 0.026$ and $b_{11} = 0.01875$ is shown in figure 5.8

The results of the simulation are presented in figure 5.8. It is possible to observe, for the case 0, case 1 and case 2 (where the initial cheater ant population does not exceed that of the worker ants), the colonies survive and stabilize at the calculated equilibrium point.

Notably in the cases where the initial cheater population does not exceed the worker population (cases 1 and 2) coexistence is achieved, while for the cases where the initial

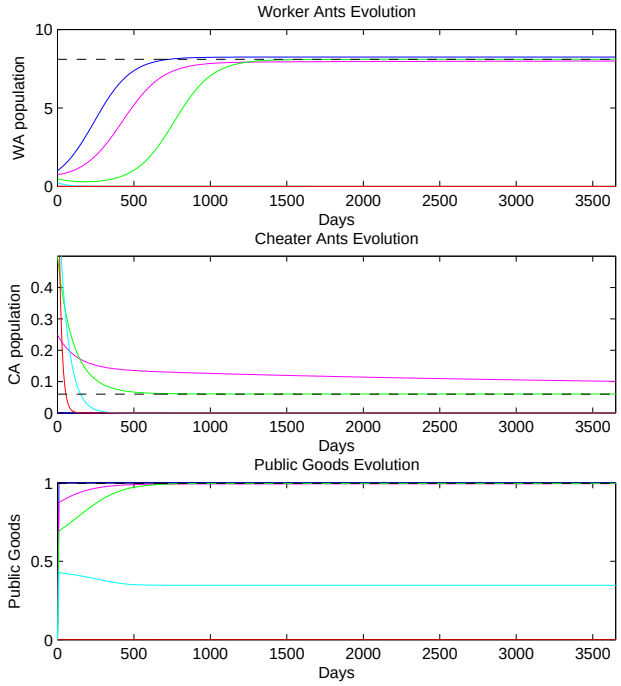

Figure 5.8: Dynamics of the model with workers uninfluenced by the cheaters with parameters $d_{21} = 0,026$ and $b_{11} = 0,01875$ in five cases format. Blue: Case 0, Pink: Case 1, Green: Case 2, Cyan: Case 3, Red: Case 4, Black: equilibrium values of P_{wu}.

setup of cheaters is larger than that of the workers (75 and 100 cheaters vs. 25 and 0 workers), extinction is the inevitable outcome. In absence of cheaters (case 0), the worker population reaches the bound imposed by overcrowding term.

Interpretation of the values to achieve coexistence

One of the possibilities to achieve coexistence varying the values of three parameters in the model, are:

- First, by eliminating dependency of worker reproduction dependency on the presence of cheaters in the nest by setting $\alpha_2 = 0$. This mean that the workers maintain their growth rate fixed with or without presence of cheaters.
- Second, the worker growth rate should increase at least 25% more.
- Finally the death rate by age (d_{21}) should be increased to a value similar to that of the death rate by starvation.

Chapter 6

Conclusions

The objectives of this dissertation were to propose a dynamic model capable of fitting the experimental data of Dobata and Tsuji [3] that presented evidence for a "public goods dilemma" between cooperator and cheater ants of the species *P. punctatus*. The starting point was an existing model of Elhanati et al. [10] in the context of cooperative protein secretion in microorganism populations, in which a heterogeneous cell population consists of two possible phenotypic states: producing and non-producing, with the former secreting protein that reacts with an external substrate to produce a resource (public good).

Several modifications to this model were proposed in order to arrive at the proposed P^3G model, as well as a more elaborate model that accounted for reproduction. This P^3G model was then fitted to the experimental data [3] using the so-called trajectory matching method, followed by a sensitivity analysis to check for the robustness of the model.

Given that the experimental data point to the eventual collapse of the colony, stability analysis of the P^3G model was carried out, to verify this for the fitted parameter values. In addition, parameter sweeps were carried out to find other parameter ranges for which coexistence is a possible outcome.

Thus the main conclusions of this dissertation can be summarized as follows:

- The proposed P^3G model, of the two predator - one prey type, using the usual tools of mathematical ecology (such as population dependency terms, Holling type responses, etc.), can be fitted to the sparse experimental data, successfully reproducing its qualitative behavior.

- The fitting of the proposed P^3G model, in the absence of data on the intermediate states of the cooperator/cheater population, could only be carried out using trajectory matching, together with a genetic algorithm, due to the relatively large

number of model parameters.

- A sensitivity analysis was carried out to test robustness of the P^3G model, but also served to identify parameters to which the trajectories are insensitive, as candidates for removal, resulting in simplification of the model. It should be mentioned that the paucity of data precluded the use of the general cross-validation and information criteria approaches.

- Stability analysis helped to show that there exist reasonable parameter ranges for which coexistence rather than extinction is the outcome.

Contributions of this dissertation

- Proposal of a new two predator - one prey model, for one of the first presentations of experimental evidence for the existence of a public goods dilemma in a social insect.

- Use of the trajectory matching method and a genetic algorithm to fit the P^3G model to a very limited amount of experimental data.

- Investigation of long-term scenarios (for which there is no experimental data) under which, for certain parameter choices, coexistence of the cooperator and cheaters speciess occurs. Such investigations might be of some use to the myrmecologists wishing to design experiments similar to those of Dobata and Tsuji.

Future work

Future work could take place along the following lines:

1. Formal proofs of positive invariance of the proposed P^3G model ODEs.

2. Investigation of conditions for the existence of globally stable behavior: equilibria or limit cycles.

3. Extension of the proposed model to study avoidance of extinction by migration or by adaptation of cheaters as reported in [31], [32]

Bibliography

[1] NOWAK, M. A. "Five rules for the evolution of cooperation", *science*, v. 314, n. 5805, pp. 1560–1563, 2006.

[2] HARDIN, G. "The tragedy of the commons", *science*, v. 162, n. 3859, pp. 1243–1248, 1968.

[3] DOBATA, S., TSUJI, K. "Public goods dilemma in asexual ant societies", *Proceedings of the National Academy of Sciences*, v. 110, n. 40, pp. 16056–16060, 2013.

[4] FEHR, E., FISCHBACHER, U. "The nature of human altruism", *Nature*, v. 425, n. 6960, pp. 785–791, 2003.

[5] MILINSKI, M. "Tit for tat in sticklebacks and the evolution of cooperation", *nature*, v. 325, n. 6103, pp. 433–435, 1987.

[6] WAKANO, J. Y., NOWAK, M. A., HAUERT, C. "Spatial dynamics of ecological public goods", *Proceedings of the National Academy of Sciences*, v. 106, n. 19, pp. 7910–7914, 2009.

[7] VELICER, G. J., KROOS, L., LENSKI, R. E. "Developmental cheating in the social bacterium Myxococcus xanthus", *Nature*, v. 404, n. 6778, pp. 598–601, 2000.

[8] DIEKERT, F. K. "Growth overfishing: the race to fish extends to the dimension of size", *Environmental and Resource Economics*, v. 52, n. 4, pp. 549–572, 2012.

[9] SIGMUND, K. *The calculus of selfishness*. Princeton University Press, 2010.

[10] ELHANATI, Y., SCHUSTER, S., BRENNER, N. "Dynamic modeling of cooperative protein secretion in microorganism populations", *Theoretical population biology*, v. 80, n. 1, pp. 49–63, 2011.

[11] STERMAN, J. D. *Business dynamics: systems thinking and modeling for a complex world*, v. 19. Irwin/McGraw-Hill Boston, 2000.

[12] KIRMAN, A. "Ants, rationality, and recruitment", *The Quarterly Journal of Economics*, pp. 137–156, 1993.

[13] GORDON, D. M. *Ant encounters: interaction networks and colony behavior*. Princeton University Press, 2010.

[14] NISHIDE, Y., SATOH, T., MURASE, K., et al. "Do Japanese queenless ants Pristomyrmex punctatus (F. Smith) exhibit genotype-based kin recognition during colony formation?" *Journal of Insect behavior*, v. 25, n. 2, pp. 137–142, 2012.

[15] BEHAR, H., BRENNER, N., LOUZOUN, Y. "Coexistence of productive and non-productive populations by fluctuation-driven spatio-temporal patterns", *Theoretical population biology*, v. 96, pp. 20–29, 2014.

[16] GORDON, D. M. *Ants at work: how an insect society is organized*. New York, Simon and Schuster, 1999.

[17] GREENE, M. J., GORDON, D. M. "Social insects: cuticular hydrocarbons inform task decisions", *Nature*, v. 423, n. 6935, pp. 32–32, 2003.

[18] ROUGHGARDEN, J. *Primer of ecological theory*. Prentice Hall Upper Saddle River, New Jersey, 1998.

[19] ALLMAN, E. S., RHODES, J. A. *Mathematical models in biology: an introduction*. Cambridge University Press, 2004.

[20] GURNEY, W., NISBET, R. M. *Ecological dynamics*. Oxford University Press, Oxford, 1998.

[21] EDELSTEIN-KESHET, L. *Mathematical models in biology*, v. 46. Siam, 1988.

[22] ABRAMS, P. A., GINZBURG, L. R. "The nature of predation: prey dependent, ratio dependent or neither?" *Trends in Ecology & Evolution*, v. 15, n. 8, pp. 337–341, 2000.

[23] BAZYKIN, A., BEREZOVSKAYA, F., DENISOV, G., et al. "The influence of predator saturation effect and competition among predators on predator-prey system dynamics", *Ecological Modelling*, v. 14, n. 1, pp. 39–57, 1981.

[24] TSUJI, K., DOBATA, S. "Social cancer and the biology of the clonal ant Pristomyrmex punctatus (Hymenoptera: Formicidae)", *Myrmecol News*, v. 15, pp. 91–99, 2011.

[25] HUNTER, A. F., DWYER, G. "Outbreaks and interacting factors: insect population explosions synthesized and dissected", *Integrative Biology: Issues, News, and Reviews*, v. 1, n. 5, pp. 166–177, 1998.

[26] HARRISON, G. W. "Comparing predator-prey models to Luckinbill's experiment with Didinium and Paramecium", *Ecology*, pp. 357–374, 1995.

[27] TURCHIN, P. *Complex population dynamics: a theoretical/empirical synthesis*, v. 35. Princeton University Press, 2003.

[28] RICHMOND, B., OTHERS. "iThink® Software V 9.0. 2. iSee SystemsâĎć". `http://www.iseesystems.com/softwares/STELLA-iThink.aspx`, 2006. [Online; accessed March-2014].

[29] CHIPPERFIELD, A., FLEMING, P., POHLHEIM, H., et al. "Genetic Algorithm TOOLBOX For Use with MATLAB". `http://www.mathworks.com/discovery/genetic-algorithm.html`, 1994. [Online; accessed January-2014].

[30] MACEY, R., OSTER, G. "Berkeley Madonna: modeling and analysis of dynamic systems". `http://www.berkeleymadonna.com/`, 2001. [Online; accessed July-2014].

[31] DOBATA, S., SASAKI, T., MORI, H., et al. "Persistence of the single lineage of transmissible "social cancer" in an asexual ant", *Molecular ecology*, v. 20, n. 3, pp. 441–455, 2011.

[32] DOBATA, S., TSUJI, K. "A cheater lineage in a social insect: Implications for the evolution of cooperation in the wild", *Communicative & integrative biology*, v. 2, n. 2, pp. 67–70, 2009.

Appendix A

Development of the smooth switching functions used in the proposed model

In a order to smooth the curves generated by the switching functions, a modification of the Holling Type II function is proposed. Consider the curve behavior of the Holling type II function, red curve in figure A.1 and the curve required in our characteristics is the inverse of it, this mean the curve approaches to its maximum value when are near to zero, as shown in the blue curve.

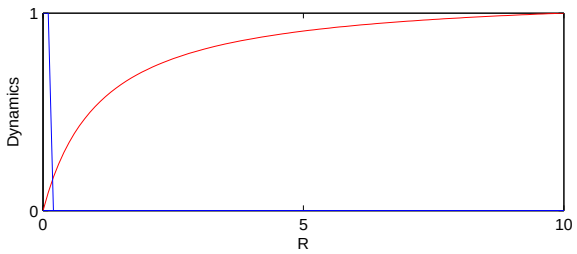

Figure A.1: Behavior of the switching function, red curve represents a typical Holling type II function, blue curve is the switching function required in the characteristics of the section 2.2.2.

To achieve this characteristic the new function is modeled though 1 as the maximum value and the subtraction of the Holling type II function, as:

$$h(R) = 1 - \frac{\beta R}{1 + \alpha R}, \tag{A.1}$$

where, R is the variable, and the second term in the right hand in the equation is the

Holling function. Resolving the equation, we obtain,

$$h(R) = \frac{1 + \alpha R - \beta R}{1 + \alpha R},$$

finally, choosing $\beta = \alpha$ we obtain the smooth switching function in (A.2), and the curve behavior for $h(R)$ is presented in the figure A.2.

$$h(R) = \frac{1}{1 + \alpha R} \tag{A.2}$$

α being the characteristic of the curve.

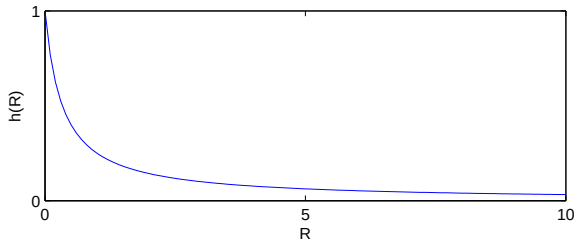

Figure A.2: Behavior of the smooth switching function $h(R)$.

Figure A.2 shows the behavior of the smooth switching function, when R is large enough $h(R)$ tends to zero, while if R tends to zero, then $h(R)$ tends to 1.

Appendix B

Materials

In the development of the model proposal, some software tools were used to solve different problems in the modeling and the stability analysis. The iThink Modeling & Simulation [28] was used to estimate the parameters, then, the Genetic Algorithms in Global Optimization Toolbox in Matlab [29] was used to fit the simulated results to the experimental results, finally Berkeley Madonna modelling software [30] was used for the seeking of coexistence in the P^3G model.

Recall that, in the simulations in long term the P^3G model is composed of three variables, while for the simulations the extended P^3G model is used composed of the five variables. Normally, in the codification of our systems is generated a flag (called of reposition switch)to switch from the P^3G model to the extended P^3G model, and with that we obtain the required flexibility at the moment of the simulations.

Ithink Model

The Ithink software was used for the first simulations to determined the dynamic of the model. Additionally the sweep tool in the curve tracer allowed the manual estimation of the parameters. The model in iThink was simulated with the integration method Runge-Kutta 4, with integration steps of 0.01. The simulation time was t in [0, 64] for the model without reposition and t in [0, 365] for the model with reposition. In the program the five cases were simulated at the same time, to compare the evolution of the populations. Figures B.1 and B.3 show the model in Ithink and figure B.2 show the graphic interface. The equations obtained from modelling in Ithink are shown in appendix F.

Genetic Algorithms Optimization

About the genetic algorithms in Matlab [29], it was used mainly for the adjustment of the best parameter values, that allows fitting the simulation results with the experimental

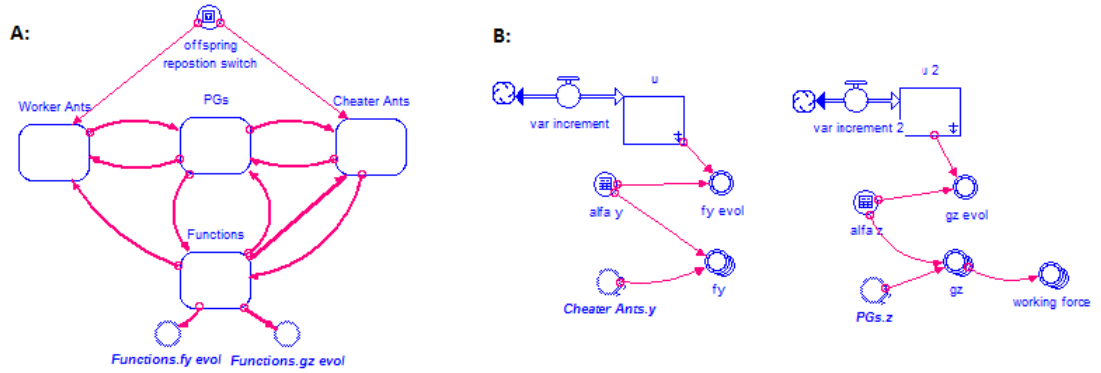

Figure B.1: Implementation of the P^3G model (2.31) in Ithink. (A) Main model by modules, (B) Module Functions, reproduction inhibition $f(y)$, starvation $g(z)$, working/recruitment force $\phi(z)$.

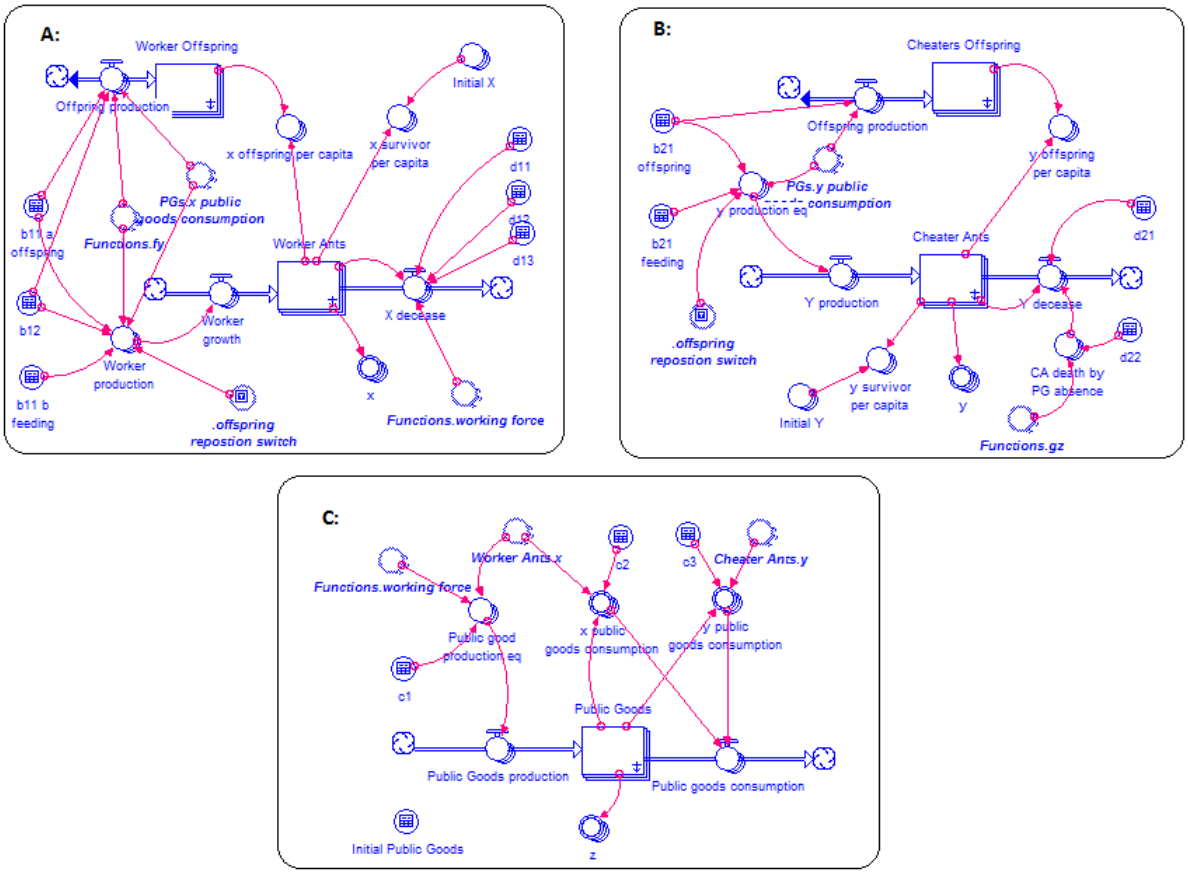

Figure B.2: Implementation of the P^3G model (2.31) in Ithink. (A) Worker ants module, (B) Cheater ants module, (C) PGs module.

curve of Dobata and Tsuji. To achieve this, the GA was configured with the following options:

- The lower bound condition was set to zero, for all the parameters.

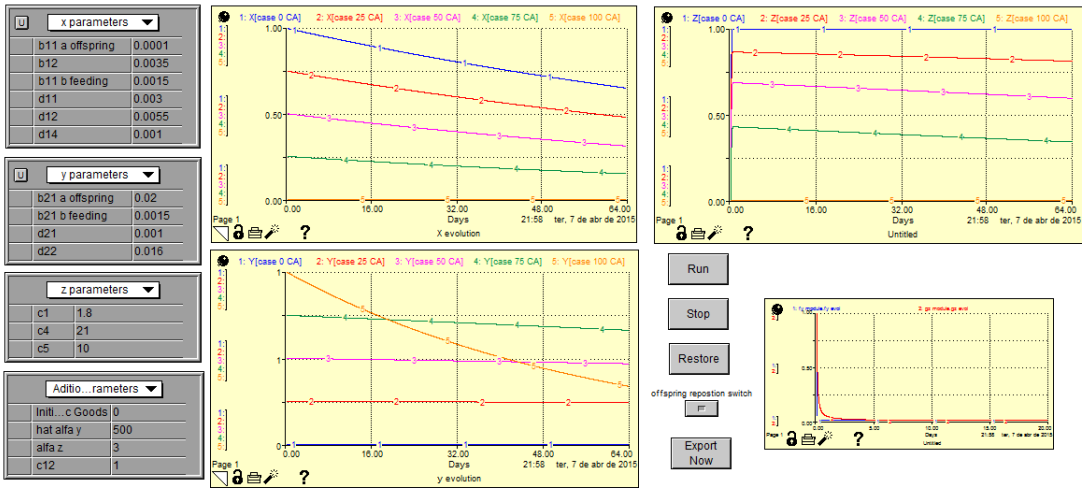

Figure B.3: Simulation interface to estimate the parameters of the P^3G model in Ithink.

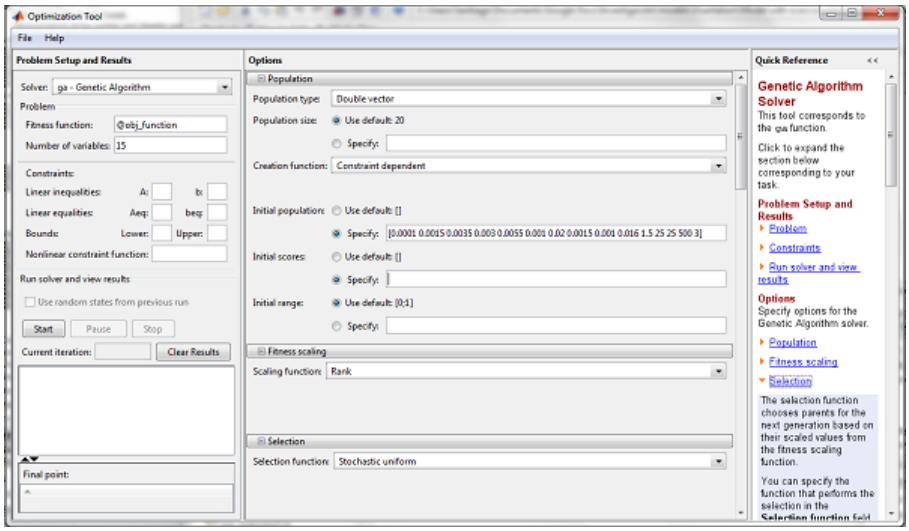

Figure B.4: Genetic algorithms tool interface to optimize the estimation of the parameters.

- The selection function was configured as Stochastic Uniform.
- The initial population is given by the vector of parameters estimated in Ithink (see appendix C for the procedure).
- The number of parameters was configured accord to the size of the vector of parameters.

The integration method used to calculate the objective function in Matlab was ODE15s, this to avoid problems of stiffness with the variation of the parameters. Figure B.4 shows the interface of the GA optimization tool.

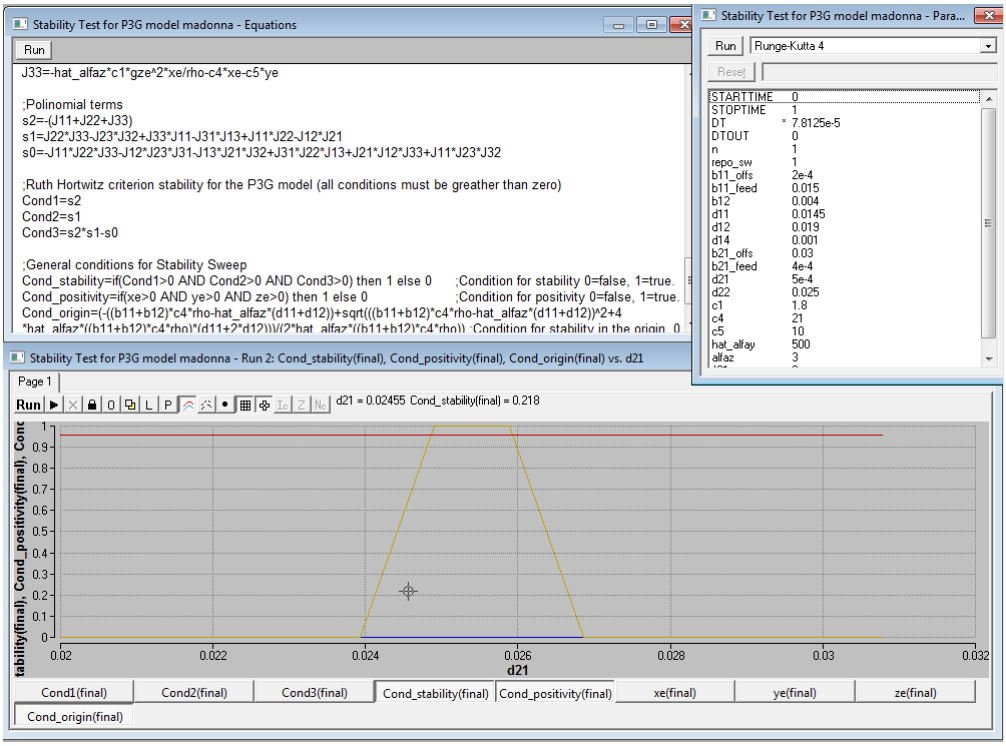

Figure B.5: Berkeley Madonna interface to sweep one parameter seeking coexistence.

Berkeley Madonna

Finally, the Berkeley Madonna software [30] was used to search coexistence in the P^3G model, since it facilitates some useful tools, like the batch of runs tool and the parameter plot tool(see figure B.5. In order to find parameters enabling coexistence in the model the differential equations of the model and the conditions for coexistence shown in appendix G, and explained in chapter 4. Later were used the parameter plot tool, and the P^3G model was simulated along the variation of one parameter to search the values that fulfill with the conditions of coexistence in the model. The data obtained from this software are plotted in figures 5.7 and 5.8.

Appendix C

Procedure to Estimate and Optimize the Parameters Values

The table with the values of the graphs of Dobata and Tsuji in [3] are in the tables C.1, C.2, C.3 and C.4.

Worker populations per capita					
Colony	Case 0	Case 1	Case 2	Case 3	Case 4
1	0.85	0.7	0.6	0.37	0
2	0.75	0.58	0.46	0.34	0
3	0.63	0.42	0.3	0.2	0
4	0.57	0.3	0.2	0.08	0
5	0.4	0.26	0.18	0	0
Mean	0.64	0.452	0.348	0.198	0
Minimum value	0.4	0.26	0.18	0	0
Maximum value	0.85	0.7	0.6	0.37	0

Table C.1: Workers population values for the experiments of Dobata and Tsuji in [3].

Offspring of the workers per capita					
Colony	Case 0	Case 1	Case 2	Case 3	Case 4
1	0.95	0.05	0.1	0	0
2	0.95	0	0.1	0	0
3	0.75	0	0.3	0	0
4	0.5	0	0	0	0
5	0	0	0	0	0
Mean	0.63	0.01	0.1	0	0
Minimum value	0	0	0	0	0
Maximum value	0.95	0.05	0.3	0	0

Table C.2: Offspring of the workers values for the experiments of Dobata and Tsuji in [3].

Cheater populations per capita					
Colony	Case 0	Case 1	Case 2	Case 3	Case 4
1	0	0.97	0.96	0.9	0.58
2	0	0.94	0.95	0.81	0.3
3	0	0.94	0.86	0.78	0.2
4	0	0.87	0.86	0.77	0.15
5	0	0.79	0.83	0.76	0
Mean	0	0.902	0.892	0.804	0.246
Minimum value	0	0.79	0.83	0.76	0
Maximum value	0	0.97	0.96	0.9	0.58

Table C.3: Cheater population values for the experiments of Dobata and Tsuji in [3].

Offspring of the cheaters per capita					
Colony	Case 0	Case 1	Case 2	Case 3	Case 4
1	0	2.1	3	1.5	0
2	0	1.7	2.3	1	0
3	0	1.25	2	0	0
4	0	0.7	1.3	0	0
5	0	0.6	0.2	0	0
Mean	0	1.27	1.76	0.5	0
Minimum value	0	0.6	0.2	0	0
Maximum value	0	2.1	3	1.5	0

Table C.4: Offspring of the workers values for the experiments of Dobata and Tsuji in [3].

The objective of this appendix is to estimate the parameters with the best values that minimize the objective function in (3.6). To achieve this, we perform some manual adjustment at first, and then, was used the Genetic Algorithm (GA) tool for optimization (refer to materials in B).

The initial parameters (initial population for the GA), were calculated manually via the Ithink software (refer to materials in B). For that, was coded the P^3G model extended (five variables) in (2.36) in Ithink, was initialized with the initial values of the populations, and configured the simulation time to t=[0,64]. Then were adjusted the parameters to meet a similar behavior that was sketched in figure 3.1. The simulation results in t=64, were compared with the mean of the experimental results for each population (refer to tables C.1, C.2, C.3 and C.4).

The initial parameters calculated in this way are shown in table C.5. Subsequently was coded the P^3G model and the objective function in Matlab, and with the use of the GA tool, were entered the initial parameters, the low bound condition (lb=0) and was ran 20 times. The results of this experience (the mean of the results and the parameters with the best score), are shown in table C.5. Additionally is shown the comparison figures

in C.1 with the first parameters optimized to visualize the results.

Results of the first experience with GA							
Param.	Initial p_0	Mean	Best vect.	Param.	Initial p_0	Mean	Best vect.
$b_{11\ offs}$	0.0001	0.0017	0.0011	c_1	1.5	1.5181	1.5466
$b_{11\ adult}$	0.0015	0.0045	0.0071	c_4	25	25.0406	25.0263
b_{12}	0.0035	0.0059	0.0066	c_5	25	25.0079	25
d_{11}	0.003	0.0052	0.0057	α_2	500	475.0157	500.0778
d_{12}	0.0055	0.0088	0.0119	α_3	26.64	14.6062	19.3277
$b_{2\ offs}$	0.02	0.0286	0.031				
$b_{2\ adult}$	0.0015	0.0037	0.0005	Fixed			
d_{21}	0.001	0.0018	0.001	d_{14}	0.001	-	-
d_{22}	0.016	0.0182	0.0183	$F(p)$	0.35	0.1457	0.1181

Table C.5: Offspring for the workers values for the experiments of Dobata and Tsuji in [3].

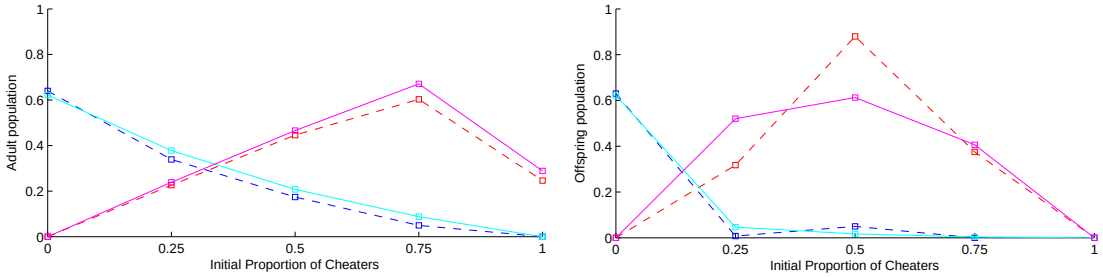

Figure C.1: Comparison between the simulation results and the experimental data first estimation of parameters for both species. (A) Proportion of surviving adults, (B) Offspring produced. Blue curve workers experimental data, cyan curve workers simulation results, red curve Cheaters experimental data, pink curve Cheaters simulation results

Results of the second experience with GA							
Param.	Initial p_0	Mean	Best vect.	Param.	Initial p_0	Mean	Best vect.
$b_{11\ offs}$	0.0002	0.0005	0.0002	α_2	500	500.006	500.0054
$b_{11\ adult}$	0.0015	0.0136	0.0145				
b_{12}	0.0066	0.0062	0.0066	Fixed			
d_{11}	0.014	0.0137	0.0119	c_1	1.8	-	-
d_{12}	0.019	0.0174	0.0207	c_4	21	-	-
$b_{2\ offs}$	0.031	0.0434	0.0441	c_5	10	-	-
$b_{2\ adult}$	0.0052	0.0043	0	α_3	26.64	-	-
d_{21}	0.0005	0.0025	0.0009	d_{14}	0.001	-	-
d_{22}	0.025	0.0231	0.0242	$F(p_0)$	0	0.1029	0.0898

Table C.6: Offspring for the workers values for the experiments of Dobata and Tsuji in [3].

Once with the best parameters, we proceeded again to a manual adjustment of some specific parameters (specially c_1, c_4, c_5, and α_3) that we detect can improve the performance of the P^3G model. Then this parameters were fixed (meaning they are not part of the optimization) and the new vector of 11 parameters to optimize was entered in the GA tool, and again was ran 20 times. The results obtained are shown in table (C.6).

After all this procedure, is confirmed that there is an improvement in the adjustment of the parameters via Genetic Algorithms, given that the objective function for the initial parameters is $(E(p_0) = 0,3500)$ and for final parameters is $E(p_{final} = 0,0898$. The simulations results with the improved parameters are shown in the figure 3.2.

Appendix D

Jacobian Components

The Jacobian matrix in (4.30) was constructed from the partial derivatives of the P^3G model in (2.31) as follows:

$$
\begin{aligned}
J_{11}(P_k) &= \frac{\delta \dot{x}}{\delta x} = \left(b_{11} + b_{12} f(y_i^*)\right) c_4 \rho_M z^* - \left(d_{11} + d_{12}\varphi(z^*) + 2d_{14} x_i^*\right); \\
J_{12}(P_k) &= \frac{\delta \dot{x}}{\delta y} = -\alpha_2 b_{12} c_4 \rho_M f(y_{j,i}^*)^2 x_i^* z^*; \\
J_{13}(P_k) &= \frac{\delta \dot{x}}{\delta z} = \left[\left(b_{11} + b_{12} f(y_i^*)\right) c_4 \rho_M + \alpha_3 w d_{12} g(z^*)^2\right] x_i^*; \\
J_{21}(P_k) &= \frac{\delta \dot{y}}{\delta x} = 0; \\
J_{22}(P_k) &= \frac{\delta \dot{y}}{\delta y} = b_2 c_5 \rho_M z^* - \left(d_{21} + d_{22} g(z^*)\right); \\
J_{23}(P_k) &= \frac{\delta \dot{y}}{\delta z} = \left[b_2 c_5 \rho_M + \alpha_3 d_{22} g(z^*)^2\right] y_i^*; \\
J_{31}(P_k) &= \frac{\delta \dot{z}}{\delta x} = c_1 \varphi(z^*) \rho_M^{-1} - c_4 z^*; \\
J_{32}(P_k) &= \frac{\delta \dot{z}}{\delta y} = -c_5 z^*; \\
J_{33}(P_k) &= \frac{\delta \dot{z}}{\delta x} = -\alpha_3 w c_1 \rho_M^{-1} g(z^*)^2 x_i^* - (c_4 x_i^* + c_5 y_i^*);
\end{aligned}
$$

Appendix E

Equilibrium points for model without the reproduction inhibition function

In this appendix are calculated the equilibrium points for the P^3G model in 2.31 with $\alpha_y = 0$, observing the model without α_2 in (5.4) still persists the equilibria in the origin with $P_{0\alpha_2} = (0, 0, z_{wd})$. The other equilibrium points are calculates next:
From (5.4), and setting $\dot{y}_{wd} = 0$, we obtain:

$$b_2 c_5 \rho_M z^*_{wd} - \left(d_{21} + \frac{d_{22}}{1 + \alpha_3 z^*_{wd}} \right) = 0$$
$$\alpha_3 b_2 c_5 \rho_M z^{*2}_{wd} + (b_2 c_5 \rho_M - \alpha_3 d_{21}) z^*_{wd} - (d_{21} + d_{22}) = 0$$

Solving the roots of the equation, we obtain the equilibrium values for z^*_{wd}

$$z^*_{i\alpha_2} = \frac{-(b_2 c_5 \rho_M - \alpha_3 d_{21}) \pm \sqrt{(b_2 c_5 \rho_M - \alpha_3 d_{21})^2 + 4\alpha_3 b_2 c_5 \rho_M (d_{21} + d_{22})}}{2\alpha_3 b_2 c_5 \rho_M}, \tag{E.1}$$

and replacing z^*_{wd} into $\varphi(\cdot)$ we obtain,

$$\varphi_i = \varphi(z^*_{i\alpha_2}) = \frac{1}{1 + \alpha_3 z^*_{i\alpha_2}}$$

Then, equating the workers equation to zero,

$$\dot{x}^*_{wd} = 0,$$
$$b_1 c_4 \rho_M z_{wd} - (d_{11} + d_{12}\varphi_i + d_{14} x^*_{wd}) = 0,$$

and isolating the x_{wd}, we obtain the equilibrium with:

$$x^*_{i\alpha_2} = \frac{b_1 c_4 \rho_M z_{wd} - (d_{11} + d_{12}\varphi_i)}{d_{14}} \tag{E.2}$$

Finally, equating to zero the PGs we obtain,

$$\begin{aligned} &\dot{z}_{wd} = 0, \\ &c_1 \varphi_i \rho_M^{-1} x^*_{i\alpha_2} - c_4 x_{i\alpha_2} z^*_{i\alpha_2} - c_5 y^*_{wd} z^*_{i\alpha_2} = 0, \end{aligned}$$

and isolating the y^*_{wd}, we obtain the final equilibrium to compound the equilibrium point in the model, with:

$$y^*_{i\alpha_2} = \frac{\left(c_1 \varphi_i \rho_M^{-1} - c_4 z^*_{i\alpha_2}\right) x^*_{i\alpha_2}}{c_5 z^*_{i\alpha_2}} \tag{E.3}$$

Appendix F

Equations in Ithink

The equations obtained from modelling in Ithink [28] are as follows:

```
P3G Model:
offspring__repostion_switch = 1

Cheater Ants:
Cheaters_Offspring[first_dimension](t) = Cheaters_Offspring[first_dimension]...
...(t - dt) + (Offspring_production[first_dimension]) * dt
INIT Cheaters_Offspring[first_dimension] = 0
INFLOWS:
Offspring_production[first_dimension] = b21_offspring*...
...PGs.y_public_goods_consumption[first_dimension]
Cheater_Ants[first_dimension](t) = Cheater_Ants[first_dimension](t - dt) +...
...(Y_production[first_dimension] - Y_decease[first_dimension]) * dt
INIT Cheater_Ants[first_dimension] = Initial_Y[first_dimension]
INFLOWS:
Y_production[first_dimension] = y_production_eq[first_dimension]
OUTFLOWS:
Y_decease[first_dimension] = (d21+CA_death_by__PG_absence[first_dimension])...
...*Cheater_Ants[first_dimension]
b21_feeding = 0.0004
b21_offspring = 0.03
CA_death_by__PG_absence[first_dimension] = d22*Functions.gz[first_dimension]
d21 = 0.0005
d22 = 0.025
Initial_Y[case_0_CA] = 0
Initial_Y[case_25_CA] = 25
```

```
Initial_Y[case_50_CA] = 50
Initial_Y[case_75_CA] = 75
Initial_Y[case_100_CA] = 100
y[first_dimension] = Cheater_Ants[first_dimension]
y_offspring__per_capita[first_dimension] = if(Cheater_Ants[first_dimension]>=1)...
...then (Cheaters_Offspring[first_dimension]/Cheater_Ants[first_dimension])...
...else(0) y_production_eq[first_dimension] = (b21_offspring...
...*.offspring__repostion_switch + b21_feeding)*...
...PGs.y_public__goods_consumption[first_dimension]
y_survivor_per_capita[first_dimension] = if(Initial_Y[first_dimension]>1)...
...then (Cheater_Ants[first_dimension]/Initial_Y[first_dimension]) else (0)

Functions:
u(t) = u(t - dt) + (var_increment) * dt
INIT u = 0
INFLOWS:
var_increment = 1
u_2(t) = u_2(t - dt) + (var_increment_2) * dt
INIT u_2 = 0
INFLOWS:
var_increment_2 = 1
alfa_y = 5
alfa_z = 3
fy[first_dimension] = 1/(1+alfa_y*Cheater_Ants.y[first_dimension])
fy_evol = 1/(1+alfa_y*u)
gz[first_dimension] = 1/(1+alfa_z*PGs.z[first_dimension])
gz_evol = 1/(1+alfa_z*u_2)
working_force[first_dimension] = 1+gz[first_dimension]

PGs:
Public_Goods[first_dimension](t) = Public_Goods[first_dimension](t - dt) +...
...(Public_Goods_production[first_dimension] -...
...Public_goods_consumption[first_dimension]) * dt
INIT Public_Goods[first_dimension] = Initial_Public_Goods
INFLOWS:
Public_Goods_production[first_dimension] =...
... Public_good__production_eq[first_dimension]
```

```
OUTFLOWS:
Public_goods_consumption[first_dimension] =...
...x_public__goods_consumption[first_dimension]...
...+y_public__goods_consumption[first_dimension]
c1 = 1.8
c2 = 0.21
c3 = 0.1
Initial_Public_Goods = 0
Public_good__production_eq[first_dimension] =...
...c1*Functions.working_force[first_dimension]*...
...Worker_Ants.x[first_dimension]
x_public__goods_consumption[first_dimension] =...
...c2*Worker_Ants.x[first_dimension]*Public_Goods[first_dimension]
y_public__goods_consumption[first_dimension] =...
...c3*Cheater_Ants.y[first_dimension]*Public_Goods[first_dimension]
z[first_dimension] = Public_Goods[first_dimension]

Worker Ants:
Worker_Ants[first_dimension](t) = Worker_Ants[first_dimension](t - dt)...
... + (Worker_growth[first_dimension] - X_decease[first_dimension]) * dt
INIT Worker_Ants[first_dimension] = Initial_X[first_dimension]
INFLOWS:
Worker_growth[first_dimension] = Worker_production[first_dimension]
OUTFLOWS:
X_decease[first_dimension] =...
...(d11+d12*Functions.working_force[first_dimension]...
... + d13*Worker_Ants[first_dimension])*Worker_Ants[first_dimension]
Worker_Offspring[first_dimension](t) =...
...Worker_Offspring[first_dimension](t - dt)...
... + (Offpring_production[first_dimension]) * dt
INIT Worker_Offspring[first_dimension] = 0
INFLOWS:
Offpring_production[first_dimension] = (b11_a_offspring...
...+ b12*Functions.fy[first_dimension])...
...*PGs.x_public__goods_consumption[first_dimension]
b11_a_offspring = 0.0002
b11_b_feeding = 0.015
```

```
b12 = 0.004
d11 = 0.0145
d12 = 0.019
d13 = 0.00001
Initial_X[case_0_CA] = 100
Initial_X[case_25_CA] = 75
Initial_X[case_50_CA] = 50
Initial_X[case_75_CA] = 25
Initial_X[case_100_CA] = 0
Worker_production[first_dimension] = ((b11_a_offspring...
...+ b12*Functions.fy[first_dimension])*.offspring__repostion_switch...
...+ b11_b_feeding)*PGs.x_public__goods_consumption[first_dimension]
x[first_dimension] = Worker_Ants[first_dimension]
x_offspring_per_capita[first_dimension] =if(Worker_Ants[first_dimension]>=1)...
...then (Worker_Offspring[first_dimension]/Worker_Ants[first_dimension])...
...else (0)
x_survivor__per_capita[first_dimension] = if (Initial_X[first_dimension]>1)...
...then (Worker_Ants[first_dimension]/Initial_X[first_dimension]) else (0)
```

Appendix G

Equations and sweep for stability in Berkeley Madonna

The equations to code the P^3G model in Berkeley Madonna are as follows:

```
;P3G Model coded in Berkeley Madonna

METHOD RK4
STARTTIME = 0
STOPTIME=64
DT = 0.01

;Some calculations
r=5 ;Five populations format
repo_sw=0;Switch of model with or without reposition 0=without, 1=with.
M=(-((c4/100)-alfaz*c1)+sqrt(((c4/100)-alfaz*c1)^2+...
...8*alfaz*(c4/100)*c1))/(2*alfaz*(c4/100)); M value calculated.

;Initializationof the variables
init_xn[1..r]=(1-0.25*(i-1))  ;workers in 5 cases format
init_yn[1..r]=0.25*(i-1) ;cheaters in 5 cases format
init_zn[1..r]=0 ;PGs

init xn[1..r]=init_xn[i] ;assignment of workers initialization
init yn[1..r]=init_yn[i] ;assignment of cheaters initialization
init zn[1..r]=init_zn[i] ;assignment of PGs initialization

init xn_offs[1..r]=0 ;Initialization of worker broods
```

```
init yn_offs[1..r]=0 ;Initialization of cheater broods

;Differential Equations
;P3G Model
d/dt(xn[1..r])=((b11_offs*repo_sw+b11_feed+b12*fyn[i]*repo_sw)*...
...c4*rho*zn[i]-(d11+d12*phin[i]+d14*xn[i]))*xn[i];workers equation
d/dt(yn[1..r])=((b21_offs*repo_sw+b21_feed)*c5*rho*zn[i]-...
...(d21+d22*gzn[i]))*yn[i] ;cheaters equation
d/dt(zn[1..r])=(c1/rho)*phin[i]*xn[i]-(c4*xn[i]+c5*yn[i])*zn[i]
;PGs equation

;Offspring equation (extended model)
d/dt(xn_offs[1..r])=(b11_offs+b12*fyn[i])*c4*rho*zn[i]*xn[i]
;workers broods equation
d/dt(yn_offs[1..r])=(b21_offs)*c5*rho*zn[i]*yn[i]
;cheaters broods equation

;Funtions
fyn[1..r]=1/(1+hat_alfay*yn[i]) ;reproduction inhibition function
gzn[1..r]=1/(1+hat_alfaz*zn[i]) ;starvation function
phin[1..r]=1+gzn[i] ;working/recruitment function

;Per capita calculations
xn_offscap[1..r]=if(xn[i]>=0.01) then (xn_offs[i]/xn[i]) else 0
yn_offscap[1..r]=if(yn[i]>=0.01) then (yn_offs[i]/yn[i]) else 0

;Parameters values
b11_offs=0.0002
b11_feed=0.015
b12=0.004
d11=0.0145
d12=0.019
d14=0.001

b21_offs=0.03
b21_feed=0.0004
d21=0.0005
```

```
d22=0.025

c1=1.8
c4=21
c5=10

hat_alfay=500
alfaz=3
hat_alfaz=alfaz*M
rho=M/100

;Calculation of the Equilibrim point
b11=b11_offs+b11_feed
b21=b21_offs+b21_feed
ze=(-(b21*c5*rho-hat_alfaz*d21)+sqrt((b21*c5*rho-hat_alfaz*d21)^2...
...+4*hat_alfaz*b21*c5*rho*(d21+d22)))/(2*hat_alfaz*b21*c5*rho)
;equilibrium in z (PGs).
gze=1/(1+hat_alfaz*ze)
phie=1+gze
e1=(hat_alfay*(c1*phie-c4*rho*ze))/(c5*rho*ze)
e2=d11+d12*phie-b11*c4*rho*ze
xe=(-(d14+e1*e2)+sqrt((d14+e1*e2)^2+4*d14*e1*(b12*c4*rho*ze-e2)))...
.../(2*d14*e1) ;equilibrium in x (worker ants).
ye=e1*xe/hat_alfay ;equilibrium in y (cheater ants).
```

And the equations to sweep the parameters seeking stability are as follows:

```
;Stability test for P3G Model

METHOD RK4
STARTTIME = 0
STOPTIME=1
DT = 0.01
n=1
repo_sw=1 ;Reposition switch 0 =without, 1 =with.
M=(-((c4/100)-alfaz*c1)+sqrt(((c4/100)-alfaz*c1)^2+...
...8*alfaz*c1*(c4/100)))/(2*alfaz*(c4/100)) ;M value calculation.
```

```
;Parameters
b11_offs=0.0002
b11_feed=0.015
b12=0.004
d11=0.0145
d12=0.019
d14=0.001

b21_offs=0.03
b21_feed=0.0004
d21=0.0005
d22=0.025

c1=1.8
c4=21
c5=10

hat_alfay=500
alfaz=3
rho=M/100
hat_alfaz=alfaz*M
b11=b11_offs+b11_feed
b21=b21_offs+b21_feed

;Equilibrum point values calculation
ze=(-(b21*c5*rho-hat_alfaz*d21)+sqrt((b21*c5*rho-hat_alfaz*d21)^2...
...+4*hat_alfaz*b21*c5*rho*(d21+d22)))/(2*hat_alfaz*b21*c5*rho)
;PGs equilibrium (positive value)
gze=1/(1+hat_alfaz*ze)
phie=1+gze
e1=(hat_alfay*(c1*phie-c4*rho*ze))/(c5*rho*ze)
e2=d11+d12*phie-b11*c4*rho*ze
xe=(-(d14+e1*e2)+sqrt((d14+e1*e2)^2+4*d14*e1*(b12*c4*rho*ze-e2)))...
.../(2*d14*e1) ;workers equilibrium (positive value)
ye=e1*xe/hat_alfay ;cheaters equilibrium
fye=1/(1+hat_alfay*ye)
```

```
;Jacobian calculation
;Partial derivates for x
J11=(b11+b12*fye)*c4*rho*ze-(d11+d12*phie+2*d14*xe)
J12=-(hat_alfay*b12*c4*rho*fye^2*xe*ze)
J13=(b11+b12*fye)*c4*rho*xe+hat_alfaz*d12*gze^2*xe

;Partial derivates for y
J21=0
J22=b21*c5*rho*ze-(d21+d22*gze)
J23=b21*c5*rho*ye+hat_alfaz*d22*gze^2*ye

;Partial derivates for z
J31=c1*phie/rho-c4*ze
J32=-c5*ze
J33=-hat_alfaz*c1*gze^2*xe/rho-c4*xe-c5*ye

;Polinomial terms
s2=-(J11+J22+J33)
s1=J22*J33-J23*J32+J33*J11-J31*J13+J11*J22-J12*J21
s0=-J11*J22*J33-J12*J23*J31-J13*J21*J32+J31*J22*J13+J21*J12*J33+...
...J11*J23*J32

;Ruth Hortwitz criterion stability for the P3G model
;(all conditions must be greater than zero)
Cond1=s2
Cond2=s1
Cond3=s2*s1-s0

;General conditions for Stability Sweep
Cond_stability=if(Cond1>0 AND Cond2>0 AND Cond3>0) then 1 else 0
;Condition for stability 0=false, 1=true.
Cond_positivity=if(xe>0 AND ye>0 AND ze>0) then 1 else 0
;Condition for positivity 0=false, 1=true.
Cond_origin=(-((b11+b12)*c4*rho-hat_alfaz*(d11+d12))+...
...sqrt(((b11+b12)*c4*rho-hat_alfaz*(d11+d12))^2+4*hat_alfaz*...
...((b11+b12)*c4*rho)*(d11+2*d12)))/(2*hat_alfaz*((b11+b12)*c4*rho))
;Condition for stability in the origin, 0=attractive, 1=repulsive.
```